Second-order stochastic theory for self-interacting scalar fields in de Sitter spacetime

Archie Cable[*] and Arttu Rajantie[†]
Department of Physics, Imperial College London, London SW7 2AZ, United Kingdom

(Received 14 September 2022; accepted 30 November 2022; published 26 December 2022)

We introduce a second-order stochastic effective theory for light scalar fields in de Sitter spacetime, extending the validity of the stochastic approach beyond the massless limit and demonstrating how it can be used to compute long-distance correlation functions nonperturbatively. The parameters of the second-order stochastic theory are determined from quantum field theory through a perturbative calculation, which is valid if the self-interaction parameter λ satisfies $\lambda \ll m^2/H^2$, where m is the scalar and H is the Hubble rate. Therefore, it allows stronger self-interactions than conventional perturbation theory, which is limited to $\lambda \ll m^4/H^4$ by infrared divergences. We demonstrate the applicability of the second-order stochastic theory by comparing its results with perturbative quantum field theory and overdamped stochastic calculations, and discuss the prospects of improving its accuracy with a full one-loop calculation of its parameters.

DOI: 10.1103/PhysRevD.106.123522

I. INTRODUCTION

Scalar quantum field theory (QFT) in de Sitter spacetime is a widely studied topic [1–4], especially in the context of inflationary cosmology [5–9]. Of particular interest is the study of the long-distance behavior of spectator scalar fields as they can lead to present-day observables with blueprints from inflation [10]. Physical examples include curvature and isocurvature perturbations [11–13], dark matter generation, [14–17], electroweak vacuum decay [18–22], and gravitational-wave background anisotropies [23].

The issue with scalar QFT in de Sitter spacetime is that self-interactions, parametrized by the coupling λ, lead to the existence of infrared divergences in perturbation theory that cannot be dealt with using standard methods beyond the limit $\lambda \ll m^4/H^4$, where m and H are the scalar mass and Hubble rate, respectively [24–27]. This is problematic when studying the long-distance behavior of these fields and has led physicists to consider alternative approaches, some of which do not require a small λ but do involve other approximations [28–39]. One such method is the stochastic approach [40,41], an effective theory where one utilizes the fact that the expansion of the inflationary spacetime causes long-wavelength modes to be stretched across the de Sitter horizon such that they can be considered classical. The remaining short-wavelength quantum modes then contribute in the form of stochastic noise. This will only be possible if m is comparable to or smaller than the horizon scale, $m \lesssim H$.

The most common application of this method is to stochastic inflation where the scalar field plays the part of the inflaton [42–69]. In this case, the fields are considered to be in slow roll such that one can use the overdamped approximation in the stochastic equations, which equates to neglecting the second derivative of the field. For this to be valid, we require the fields to be light ($m \ll H$) and for the coupling to be sufficiently small ($\lambda \ll m^2/H^2$). In this limit, one can derive the overdamped stochastic equations by introducing a cutoff between sub- and superhorizon field modes with a strict boundary [40,41]. The superhorizon modes then play the role of a classical field while the subhorizon "quantum" modes contribute via a stochastic white noise. This mode expansion derivation has been widely studied [42–57,70,71] alongside an alternative path-integral approach that aligns more with standard thermal field theory methods [53,58–69].

The stochastic approach has not exclusively been applied to the inflaton. From the seminal work of Starobinsky and Yokoyama [40,41] to more recent applications to inflationary observables [16,17,70–72], there are examples of the stochastic approach being applied to spectator scalar fields. In this case, the slow-roll condition can be relaxed and one should consider the full second-order stochastic equations. However, in our previous paper [72], we showed that for free fields the standard cutoff procedure cannot be used to derive the second-order stochastic equations when one goes beyond the limit $m \ll H$. This is not a fault in the stochastic equations themselves, but rather in the

[*]archie.cable18@imperial.ac.uk
[†]a.rajantie@imperial.ac.uk

expression for the noise amplitude that one computes using a cutoff. Given the correct form of the noise, the quantum correlators can be recovered from these second-order equations. Following the standard technique for effective field theories, this form was found by evaluating the stochastic field correlator for an unspecified noise amplitude and then matching with the quantum field propagator in order to determine the desired noise amplitude. This suggests that the stochastic approach is still viable away from the overdamped limit but the strict cutoff procedure is no longer a valid means of deriving the stochastic equations from the underlying quantum theory.

In this paper, we take this idea a step further and introduce interactions into the stochastic equations. We relax the overdamped approximation that $m \ll H$ to show that in perturbation theory we can once again use the matching procedure to find the forms of the stochastic parameters—namely, the mass, coupling, and noise amplitudes—that reproduce the quantum correlators. Further, we present a numerical method for solving the second-order stochastic equations such that stochastic correlation functions can be found nonperturbatively.

The results we obtain using the second-order stochastic effective theory in this work are valid for fields with mass $m \lesssim H$ and quartic self-interaction coupling $\lambda \ll m^2/H^2$. We leave it to future work [73] to compute $\mathcal{O}(\frac{\lambda H^2}{m^2})$ contributions, where we will have to employ a renormalization scheme in QFT in order to compute the stochastic noise amplitudes. However, we are already going beyond perturbative techniques in QFT and the overdamped approximation, which are only valid in the regimes $\lambda \ll m^4/H^4$ and $m \ll H$, respectively. The second-order stochastic approach encompasses these regions and goes further where it can compute physical results that the established approximations cannot.

The paper is organized as follows. In Sec. II we review the status of perturbative QFT and discuss how infrared divergences limit its computational power, focusing on a self-interacting theory with quartic coupling. In Sec. III we briefly summarize the overdamped stochastic approach before introducing the second-order stochastic equations. We introduce a spectral expansion method to compute stochastic correlators and give the forms of these in terms of the eigenspectrum. In Sec. IV we begin by summarizing the results from Ref. [72] for free fields before using perturbation theory to compute stochastic correlators to leading order in the self-interaction coupling. We compare these results to their equivalents at $\mathcal{O}(\frac{\lambda H^4}{m^4})$ in perturbative QFT, from which we find the values of the stochastic parameters required to reproduce the quantum result. In Sec. V we outline the numerical method to evaluate correlators nonperturbatively and then, using the noise functions found in Sec. IV, we perform a full comparison between the second-order stochastic, overdamped stochastic, and perturbative QFT approaches. Finally, we discuss the results and conclude in Sec. VI.

II. QUANTUM FIELD THEORY IN DE SITTER SPACETIME

We begin by reviewing the status of scalar QFT in de Sitter spacetime, focusing on the calculation of the Feynman propagator. We consider a spectator scalar field $\phi(t,\mathbf{x})$ with scalar potential $V(\phi)$ on a de Sitter background with scale factor $a(t) = e^{Ht}$. $H = \dot{a}/a$ is the Hubble rate which will be kept constant throughout. Introducing the field momentum $\pi(t,\mathbf{x})$, we can write the equations of motion as

$$\begin{pmatrix} \dot{\phi} \\ \dot{\pi} \end{pmatrix} = \begin{pmatrix} \pi \\ -3H\pi - V'(\phi) \end{pmatrix}, \tag{1}$$

where primes and dots denote derivatives with respect to ϕ and t, respectively. We focus on a ϕ^4 theory such that the potential $V(\phi) = \frac{1}{2}m^2\phi^2 + \frac{1}{4}\lambda\phi^4$, where m is the scalar mass and λ is the quartic coupling constant. We introduce a nonminimal coupling to gravity ξ, which is included in the scalar mass term as $m^2 = m_0^2 + 12\xi H^2$.

A. Free quantum fields

For free fields ($\lambda = 0$), one can follow standard QFT procedures to calculate the Feynman propagator, resulting in [1–4]

$$\begin{aligned} i\Delta(t,t',\mathbf{x},\mathbf{x}') &\coloneqq \langle \hat{T}\hat{\phi}(t,\mathbf{x})\hat{\phi}(t',\mathbf{x}')\rangle \\ &= \frac{H^2}{16\pi^2}\Gamma\left(\frac{3}{2}+\nu\right)\Gamma\left(\frac{3}{2}-\nu\right){}_2F_1\left(\frac{3}{2}+\nu,\frac{3}{2}-\nu,2;1+\frac{y}{2}\right) \end{aligned} \tag{2}$$

in the Bunch-Davies vacuum, where ${}_2F_1(a,b,c;z)$ is the hypergeometric function, $\Gamma(z)$ are the Euler-gamma functions, $\nu = \sqrt{\frac{9}{4} - \frac{m^2}{H^2}}$, and y is the spacetime interval given by

$$y = \cosh(H(t-t')) - \frac{H^2}{2}a(t)a(t')|\mathbf{x}-\mathbf{x}'|^2 - 1. \tag{3}$$

We can instead write the Feynman propagator as

$$i\Delta(t,t',\mathbf{x},\mathbf{x}') = \frac{H^2}{16\pi^2}\left[\frac{\Gamma(2\nu)\Gamma(1-2\nu)}{\Gamma(\frac{1}{2}+\nu)\Gamma(\frac{1}{2}-\nu)}\sum_{n=0}^{\infty}\frac{\Gamma(\frac{3}{2}-\nu+n)\Gamma(\frac{1}{2}-\nu+n)}{\Gamma(1-2\nu+n)n!}\left(-\frac{y}{2}\right)^{-\frac{3}{2}+\nu-n} + \frac{\Gamma(-2\nu)\Gamma(1+2\nu)}{\Gamma(\frac{1}{2}+\nu)\Gamma(\frac{1}{2}-\nu)}\sum_{n=0}^{\infty}\frac{\Gamma(\frac{3}{2}+\nu+n)\Gamma(\frac{1}{2}+\nu+n)}{\Gamma(1+2\nu+n)n!}\left(-\frac{y}{2}\right)^{-\frac{3}{2}-\nu-n}\right], \tag{4}$$

which allows us to see the behavior as a function of large spacetime separations. Explicitly, the leading IR behavior of the free Feynman propagator is

$$i\Delta(t,t,\mathbf{0},\mathbf{x}) = \frac{H^2}{16\pi^2}\frac{\Gamma(\frac{3}{2}-\nu)\Gamma(2\nu)4^{\frac{3}{2}-\nu}}{\Gamma(\frac{1}{2}+\nu)}|Ha(t)\mathbf{x}|^{-\frac{3}{2}+\nu}, \tag{5}$$

where we have focused on the equal-time propagator. It is this behavior that one would expect the stochastic approach to reproduce for free fields.

B. Perturbative QFT

Introducing interactions is a challenging process; the Feynman propagator cannot be found for all values of m and λ using current techniques, namely, perturbation theory. However, one can still obtain useful results. In perturbative ϕ^4 theory, the only contribution at first-order λ is the tadpole diagram; therefore, there is no field renormalization and the only contribution comes via a mass correction, where the bare mass m is replaced by an effective mass $m_{Q\mathrm{eff}}$ via

$$m^2 \to m_{Q\mathrm{eff}}^2 = m^2 + 3\lambda\langle\hat{\phi}^2\rangle. \tag{6}$$

One can therefore obtain the resummed one-loop Feynman propagator by replacing m with $m_{Q\mathrm{eff}}$ in Eq. (2). The leading IR behavior is given by

$$i\Delta(t,t',\mathbf{x},\mathbf{x}') = \frac{H^2}{16\pi^2}\frac{\Gamma(\frac{3}{2}-\nu_{Q\mathrm{eff}})\Gamma(2\nu_{Q\mathrm{eff}})}{\Gamma(\frac{1}{2}+\nu_{Q\mathrm{eff}})}\left(-\frac{y}{2}\right)^{-\frac{3}{2}+\nu_{Q\mathrm{eff}}}, \tag{7}$$

where $\nu_{Q\mathrm{eff}} = \sqrt{\frac{9}{4}-\frac{m_{Q\mathrm{eff}}^2}{H^2}}$. In practice, this is problematic as $\langle\hat{\phi}^2\rangle$ contains divergences at $\mathcal{O}(\lambda)$. To see this, we expand Eq. (2) for $y \to 0$ such that the field variance is given by

$$\begin{aligned}\langle\hat{\phi}^2\rangle &= \lim_{y\to 0} i\Delta(t,t',\mathbf{x},\mathbf{x}') \\ &= -\frac{H^2}{8\pi^2 y} + \frac{m^2-2H^2}{16\pi^2}\bigg(\ln y + i\pi - 1 + 2\gamma_E - \ln 2 \\ &\quad + \psi^{(0)}\left(\frac{3}{2}-\nu\right) + \psi^{(0)}\left(\frac{3}{2}+\nu\right)\bigg),\end{aligned} \tag{8}$$

where $\psi^{(0)}(z)$ are the polygamma functions and γ_E is the Euler-Mascheroni constant. We see that the $\mathcal{O}(1/y)$ and $\mathcal{O}(\ln y)$ are UV divergent. Such terms are removed by introducing a renormalized mass $m_R^2 = m_{0,R}^2 + 12\xi_R H^2$ such that the divergent $\mathcal{O}(m^2)$ and $\mathcal{O}(H^2)$ are renormalized by the $m_{0,R}$ and ξ_R parameters, respectively. Expanding the finite part to leading order in mass, the UV-finite effective mass is given by [62]

$$m_{Q\mathrm{eff}}^2 = m_R^2 + \frac{9\lambda H^4}{8\pi^2 m_R^2} + \mathcal{O}(\lambda H^2), \tag{9}$$

where the $\mathcal{O}(\lambda H^2)$ part will include terms that are dependent on the renormalization scheme. This expression tells us that there also exists an IR divergence in the theory since the leading term in the small-mass expansion is of relative order $\mathcal{O}(\frac{\lambda H^4}{m^4})$, which is large if $m \ll \lambda^{1/4}H$, and therefore perturbative QFT is only valid in the limit $\lambda \ll m^4/H^4$; the additional finite terms in Eq. (9) are unimportant. Thus, the leading term in the spacelike Feynman propagator is

$$i\Delta(t,t,\mathbf{0},\mathbf{x}) = \left(\frac{H^2}{16\pi^2}\frac{\Gamma(\frac{3}{2}-\nu)\Gamma(2\nu)4^{\frac{3}{2}-\nu}}{\Gamma(\frac{1}{2}+\nu)} - \frac{27\lambda H^8}{64\pi^4 m_R^6} + \mathcal{O}\left(\frac{\lambda H^6}{m_R^4}\right)\right)|Ha(t)\mathbf{x}|^{-\frac{2\Lambda_1^{(\mathrm{QFT})}}{H}}, \tag{10}$$

where

$$\Lambda_1^{(\mathrm{QFT})} = \left(\frac{3}{2}-\nu\right)H + \frac{3\lambda H^3}{8\pi^2 m_R^2} + \mathcal{O}(\lambda H). \tag{11}$$

It is because of these IR divergences that we pursue other methods of computing correlators in de Sitter spacetime, such as the stochastic approach, in order to go beyond the limit where $\lambda \ll m^4/H^4$.

III. STOCHASTIC APPROACH

A. Overdamped stochastic approach

The seminal work of Starobinsky and Yokoyama [40,41] introduced an effective theory for scalar fields in de Sitter spacetime which goes beyond the perturbative methods introduced above. We call this the overdamped (OD) stochastic approach. The principle is that one can separate the short- and long-wavelength modes of the scalar field such that the short-wavelength modes contribute a stochastic noise to the classical equations of motion. Thus, we obtain the IR behavior of the fields. In the overdamped limit

$\dot{\pi} \ll 3H\pi$ and $V''(\phi) \ll H^2$, one can derive the stochastic equations from the underlying QFT by introducing a strict cutoff between long- and short-wavelength modes, resulting in the OD stochastic equation

$$\dot{\phi} + \frac{V'(\phi)}{3H} = \xi_{\mathrm{OD}} \tag{12}$$

with a white-noise contribution $\xi_{\mathrm{OD}}(t, \mathbf{x})$ with correlation

$$\langle \xi_{\mathrm{OD}}(t, \mathbf{x}) \xi_{\mathrm{OD}}(t', \mathbf{x}) \rangle = \frac{H^3}{4\pi^2} \delta(t - t'). \tag{13}$$

From this starting point, one can do fully nonperturbative calculations to find stochastic correlators that go beyond perturbative QFT. The details of this calculation were given in Ref. [70] where the authors used a spectral expansion method to perform their computation. To compare this approach with QFT, we write the spacelike OD stochastic field correlator to one-loop order as

$$\langle \phi(t, \mathbf{0}) \phi(t, \mathbf{x}) \rangle = \left(\frac{3H^4}{8\pi^2 m^2} - \frac{27\lambda H^8}{64\pi^4 m^6} + \mathcal{O}(\lambda^2) \right) |Ha(t)\mathbf{x}|^{-\frac{2\Lambda_1^{(\mathrm{OD})}}{H}}, \tag{14}$$

where

$$\Lambda_1^{(\mathrm{OD})} = \frac{m^2}{3H} + \frac{3\lambda H^3}{8\pi^2 m^2} + \mathcal{O}(\lambda^2). \tag{15}$$

Comparing this to the Feynman propagator (10), we see that there will only be agreement in the limit where $m \ll H$. The OD stochastic approach does not reproduce the full expression for the free part of the Feynman propagator, nor will it include any terms of relative order $\mathcal{O}(\frac{\lambda H^2}{m^2})$ since the next order in the perturbative expansion goes straight to $\mathcal{O}(\lambda^2)$. Thus, the OD stochastic approach is only valid in the regime $\lambda \ll m^2/H^2$.

B. Second-order stochastic equations

For the cosmological applications of spectator fields in de Sitter spacetime, we wish to go beyond the OD approximation where $m^2 \ll H^2$. To do this, we introduce second-order stochastic equations; however, the standard cutoff procedure used to derive the OD stochastic equation is no longer valid when the fields become more massive [72]. Instead of attempting a derivation from the underlying QFT, we introduce a top-down method where we derive stochastic correlation functions from a stochastic equation and then show that these can reproduce their quantum counterparts given the appropriate choice of stochastic parameters. Taking inspiration from Eq. (1), we write the second-order stochastic equation as

$$\begin{pmatrix} \dot{\phi} \\ \dot{\pi} \end{pmatrix} = \begin{pmatrix} \pi \\ -3H\pi - V'(\phi) \end{pmatrix} + \begin{pmatrix} \xi_\phi \\ \xi_\pi \end{pmatrix}, \tag{16}$$

where the potential is given by

$$V(\phi) = \frac{1}{2} m^2 \phi^2 + \frac{1}{4} \lambda \phi^4 \tag{17}$$

and the stochastic white-noise contributions $\xi_i(t, \mathbf{x})$, $i \in \{\phi, \pi\}$ satisfy

$$\langle \xi_i(t, \mathbf{x}) \xi_j(t', \mathbf{x}) \rangle = \sigma_{ij}^2 \delta(t - t'). \tag{18}$$

The parameters of the stochastic theory are m, λ, and σ_{ij}^2. In this paper, we determine their relation to QFT parameters using perturbation theory. Since the perturbative expansion is in powers of λ, we assume that the couplings in the stochastic approach and perturbative QFT are the same. On the other hand, m and σ_{ij}^2 will be determined by matching stochastic correlators to their QFT counterparts.

Now that we have a stochastic theory, we introduce the one-point probability distribution function (1PDF) in phase space $P(\phi, \pi; t)$. Its time evolution is described by the Fokker-Planck equation

$$\begin{aligned} \partial_t P(\phi, \pi; t) &= \Big[3H - \pi \partial_\phi + (3H\pi + V'(\phi)) \partial_\pi + \frac{1}{2} \sigma_{\phi\phi}^2 \partial_\phi^2 \\ &\quad + \sigma_{\phi\pi}^2 \partial_\phi \partial_\pi + \frac{1}{2} \sigma_{\pi\pi}^2 \partial_\pi^2 \Big] P(\phi, \pi; t) \\ &= \mathcal{L}_{FP} P(\phi, \pi; t), \end{aligned} \tag{19}$$

where $\mathcal{L}_{FP}$ is called the Fokker-Planck operator.

C. Spectral expansion

For free fields, one can solve the Fokker-Planck equation (19) analytically via a spectral expansion [72]. The introduction of self-interactions will result in the need for numerical calculations but one can still use the spectral expansion for the basis of these computations.

We define a space of functions $\{f | (f, f) < \infty\}$ with the scalar product

$$(f, g) = \int_{-\infty}^{\infty} d\phi \int_{-\infty}^{\infty} d\pi f(\phi, \pi) g(\phi, \pi). \tag{20}$$

Note that all integrals over ϕ and π have the above limits unless otherwise stated. There then exists an adjoint to the Fokker-Planck operator, $\mathcal{L}_{\mathrm{FP}}^*$, which is defined via

$$(\mathcal{L}_{\mathrm{FP}} f, g) = (f, \mathcal{L}_{\mathrm{FP}}^* g). \tag{21}$$

Explicitly, the adjoint Fokker-Planck operator is

$$\mathcal{L}_{\rm FP}^{*} = \pi\partial_\phi - (3H\pi + V'(\phi))\partial_\pi + \frac{1}{2}\sigma_{\phi\phi}^2\partial_\phi^2 + \sigma_{\phi\pi}^2\partial_\phi\partial_\pi + \frac{1}{2}\sigma_{\pi\pi}^2\partial_\pi^2. \tag{22}$$

The 1PDF can be written as

$$P(\phi,\pi;t) = \Psi_0^*(\phi,\pi)\sum_{N=0}^{\infty}\Psi_N(\phi,\pi)e^{-\Lambda_N t}, \tag{23}$$

where Λ_N and $\Psi_N^{(*)}(\phi,\pi)$ are the respective eigenvalues and (adjoint) eigenvectors to the (adjoint) Fokker-Planck operator,

$$\mathcal{L}_{\rm FP}\Psi_N(\phi,\pi) = -\Lambda_N\Psi_N(\phi,\pi), \tag{24a}$$

$$\mathcal{L}_{\rm FP}^*\Psi_N^*(\phi,\pi) = -\Lambda_N\Psi_N^*(\phi,\pi). \tag{24b}$$

The eigenvectors obey the biorthogonality and completeness relations

$$(\Psi_N^*,\Psi_{N'}) = \delta_{N'N}, \tag{25a}$$

$$\sum_N \Psi_N^*(\phi,\pi)\Psi_N(\phi',\pi') = \delta(\phi-\phi')\delta(\pi-\pi'), \tag{25b}$$

and there exists an equilibrium state $P_{\rm eq}(\phi,\pi) = \Psi_0^*(\phi,\pi)\Psi_0(\phi,\pi)$ obeying $\partial_t P_{\rm eq}(\phi,\pi) = 0$.

D. Stochastic correlators

To obtain stochastic correlators, we introduce the transfer matrix $U(\phi_0,\phi,\pi_0,\pi;t)$ between $(\phi_0,\pi_0) = (\phi(0,\mathbf{x}),\pi(0,\mathbf{x}))$ and $(\phi,\pi) = (\phi(t,\mathbf{x}),\pi(t,\mathbf{x}))$, which is defined as the Green's function of the Fokker-Planck equation, i.e.,

$$\partial_t U(\phi_0,\phi,\pi_0,\pi) = \mathcal{L}_{\rm FP}U(\phi_0,\phi,\pi_0,\pi;t) \tag{26}$$

for all values of ϕ_0 and π_0. Then, the time dependence of the 1PDF is given by

$$P(\phi,\pi;t) = \int d\phi_0\int d\pi_0 P(\phi_0,\pi_0;0)U(\phi_0,\phi,\pi_0,\pi;t). \tag{27}$$

From Eq. (23), making use of the relations (25), we find that the transfer matrix can be written with the spectral expansion as

$$U(\phi_0,\phi,\pi_0,\pi;t) = \frac{\Psi_0^*(\phi,\pi)}{\Psi_0^*(\phi_0,\pi_0)}\sum_N\Psi_N^*(\phi_0,\pi_0)\Psi_N(\phi,\pi)e^{-\Lambda_N t} \tag{28}$$

and in turn we can write a two-point probability distribution function (2PDF) as

$$\begin{aligned} P_2(\phi_0,\phi,\pi_0,\pi;t) &= P_{\rm eq}(\phi_0,\pi_0)U(\phi_0,\phi,\pi_0,\pi;t) \\ &= \Psi_0^*(\phi,\pi)\Psi_0(\phi_0,\pi_0)\sum_N\Psi_N^*(\phi_0,\pi_0)\Psi_N(\phi,\pi)e^{-\Lambda_N t}. \end{aligned} \tag{29}$$

The two-point timelike (equal-space) stochastic correlator between some functions $f(\phi_0,\pi_0)$ and $g(\phi,\pi)$ is given by

$$\begin{aligned} \langle f(\phi_0,\pi_0)g(\phi,\pi)\rangle &= \int d\phi_0\int d\phi\int d\pi_0 \\ &\quad\times\int d\pi P_2(\phi_0,\phi,\pi_0,\pi;t)f(\phi_0,\pi_0)g(\phi,\pi) \\ &= \sum_N f_N^* g_N e^{-\Lambda_N t}, \end{aligned} \tag{30}$$

where

$$f_N^* = (\Psi_0 f,\Psi_N^*), \tag{31a}$$

$$g_N = (\Psi_N g,\Psi_0^*). \tag{31b}$$

In a similar vein to the 2PDF, we can write a three-point probability distribution function (3PDF) between points (ϕ_0,π_0), (ϕ_1,π_1), and (ϕ_2,π_2) as

$$\begin{aligned} P_3(\phi_0,\phi_1,\phi_2,\pi_0,\pi_1,\pi_2;t_1,t_2) &= P_{\rm eq}(\phi_0,\pi_0)U(\phi_0,\phi_1,\pi_0,\pi_1;t_1)U(\phi_0,\phi_2,\pi_0,\pi_2;t_2) \\ &= \frac{\Psi_0(\phi_0,\pi_0)\Psi_0^*(\phi_1,\pi_1)\Psi_0^*(\phi_2,\pi_2)}{\Psi_0^*(\phi_0,\pi_0)} \\ &\quad\times\sum_N\Psi_N^*(\phi_0,\pi_0)\Psi_N(\phi_1,\pi_1) \\ &\quad\times\sum_{N'}\Psi_{N'}^*(\phi_0,\pi_0)\Psi_{N'}(\phi_2,\pi_2)e^{-(\Lambda_N t_1+\Lambda_{N'}t_2)}. \end{aligned} \tag{32}$$

To evaluate the spacelike (equal-time) stochastic correlators, we follow Ref. [41] and introduce the time coordinate t_r at which the comoving $\mathbf{x}_1$ and $\mathbf{x}_2$ are inside the same Hubble volume,

$$t_r = -\frac{1}{H}\ln(H|\mathbf{x}_2-\mathbf{x}_1|). \tag{33}$$

Using the 3PDF $P_3(\phi_r,\phi_1,\phi_2,\pi_r,\pi_1,\pi_2)$, the spacelike stochastic correlator between the functions $f(\phi(t,\mathbf{x}_1),\pi(t,\mathbf{x}_1))$ and $g(\phi(t,\mathbf{x}_2),\pi(t,\mathbf{x}_2))$ is given by integrating over ϕ_r and π_r as

$$\begin{aligned}&\langle f(\phi,\pi;t,\mathbf{x}_1)g(\phi,\pi;t,\mathbf{x}_2)\rangle\\&=\int d\phi_r\int d\phi_1\int d\phi_2\int d\pi_r\int d\pi_1\int d\pi_2 P_3(\phi_r,\phi_1,\phi_2,\pi_r,\pi_1,\pi_2)f(\phi_1,\pi_1)g(\phi_2,\pi_2)\\&=\int d\phi_r\int d\pi_r\frac{\Psi_0(\phi_r,\pi_r)}{\Psi_0^*(\phi_r,\pi_r)}\sum_{NN'}\Psi_N^*(\phi_r,\pi_r)\Psi_{N'}^*(\phi_r,\pi_r)f_N g_{N'}|Ha(t)(\mathbf{x}_1-\mathbf{x}_2)|^{-\frac{\Lambda_N+\Lambda_{N'}}{H}}.\end{aligned} \tag{34}$$

IV. COMPARISON WITH PERTURBATIVE QFT

A. Free field theory

We now have a formalism that can be used to calculate stochastic correlators but we have yet to attribute it to anything physical as we have not yet specified the noise amplitudes. We now compare it with the QFT results from Sec. II, starting with free fields. This case was studied in full in Ref. [72] so this section will be a review.

It will prove convenient to change our field variables from (ϕ,π) to (q,p), with the transformation

$$\begin{pmatrix}p\\q\end{pmatrix}=\frac{1}{\sqrt{1-\frac{\alpha}{\beta}}}\begin{pmatrix}1&\alpha H\\\frac{1}{\beta H}&1\end{pmatrix}\begin{pmatrix}\pi\\\phi\end{pmatrix}, \tag{35}$$

where $\alpha=\frac{3}{2}-\nu$ and $\beta=\frac{3}{2}+\nu$. All of the formalism introduced in the previous section can also be applied to (q,p) variables. In particular, the Fokker-Planck operators are given by

$$\mathcal{L}_{\rm FP}=\mathcal{L}_{\rm FP}^{(0)}+\lambda\mathcal{L}_{\rm FP}^{(1)}, \tag{36a}$$

$$\mathcal{L}_{\rm FP}^{*}=\mathcal{L}_{\rm FP}^{(0)*}+\lambda\mathcal{L}_{\rm FP}^{(1)*}, \tag{36b}$$

where the free part is given by

$$\begin{aligned}\mathcal{L}_{\rm FP}^{(0)}&=\alpha H+\alpha Hq\partial_q+\frac{1}{2}\sigma_{qq}^2\partial_q^2+\beta H+\beta Hp\partial_p\\&\quad+\frac{1}{2}\sigma_{pp}^2\partial_p^2+\sigma_{qp}^2\partial_q\partial_p,\end{aligned} \tag{37a}$$

$$\mathcal{L}_{\rm FP}^{(0)*}=-\alpha Hq\partial_q+\frac{1}{2}\sigma_{qq}^2\partial_q^2-\beta Hp\partial_p+\frac{1}{2}\sigma_{pp}^2\partial_p^2+\sigma_{qp}^2\partial_q\partial_p \tag{37b}$$

and the interacting part is given by

$$\mathcal{L}_{\rm FP}^{(1)}=\frac{\lambda}{(1-\frac{\alpha}{\beta})^2}\left(-\frac{1}{\beta H}p+q\right)^3\left(\partial_p+\frac{1}{\beta H}\partial_q\right), \tag{38a}$$

$$\mathcal{L}_{\rm FP}^{(1)*}=-\mathcal{L}_{\rm FP}^{(1)}. \tag{38b}$$

The (q,p) noise amplitudes are written in terms of their (ϕ,π) counterparts as

$$\sigma_{qq}^2=\frac{1}{1-\frac{\alpha}{\beta}}\left(\frac{1}{\beta^2H^2}\sigma_{\pi\pi}^2+\frac{2}{\beta H}\sigma_{\phi\pi}^2+\sigma_{\phi\phi}^2\right), \tag{39a}$$

$$\sigma_{qp}^2=\frac{1}{1-\frac{\alpha}{\beta}}\left(\frac{1}{\beta H}\sigma_{\pi\pi}^2+\left(1+\frac{\alpha}{\beta}\right)\sigma_{\phi\pi}^2+\alpha H\sigma_{\phi\phi}^2\right), \tag{39b}$$

$$\sigma_{pp}^2=\frac{1}{1-\frac{\alpha}{\beta}}(\sigma_{\pi\pi}^2+2\alpha H\sigma_{\phi\pi}^2+\alpha^2H^2\sigma_{\phi\phi}^2). \tag{39c}$$

Further, the $\phi-\phi$ correlator is written in terms of the (q,p) correlators as

$$\begin{aligned}&\langle\phi(t,\mathbf{x})\phi(t',\mathbf{x}')\rangle\\&=\frac{1}{1-\frac{\alpha}{\beta}}\left(\frac{1}{\beta^2H^2}\langle p(t,\mathbf{x})p(t',\mathbf{x}')\rangle-\frac{1}{\beta H}\langle q(t,\mathbf{x})p(t',\mathbf{x}')\rangle\right.\\&\quad\left.-\frac{1}{\beta H}\langle p(t,\mathbf{x})q(t',\mathbf{x}')\rangle+\langle q(t,\mathbf{x})q(t',\mathbf{x}')\rangle\right).\end{aligned} \tag{40}$$

Similar expressions can be found for the $\phi-\pi$, $\pi-\phi$, and $\pi-\pi$ correlators but we will focus on the $\phi-\phi$ correlator in this work. Following the work of Ref. [72], we compute the stochastic free field correlator and match it to the free Feynman propagator (5) to obtain an expression for the noise amplitudes, resulting in

$$\sigma_{qq}^{2(0)}=\frac{2H^3\Gamma(1+\nu)\Gamma\left(\frac{5}{2}-\nu\right)}{\pi^{5/2}(3+2\nu)}, \tag{41a}$$

$$\sigma_{qp}^{2(0)}=0, \tag{41b}$$

$$\sigma_{pp}^{2(0)}=0. \tag{41c}$$

The qq noise is matched such that the leading-order term in the Feynman propagator is reproduced and the qp noise is chosen such that there is an analytic continuation from timelike to spacelike stochastic correlators, a behavior prevalent in QFT. However, the choice of σ_{pp}^2 is arbitrary. In this paper, we set it to zero—the subleading term does not contribute—because it is the simplest case. The (q,p) noise matrix contains a zero eigenvalue and thus one would expect the stochastic equations to simplify, though we do not pursue this here.

In Ref. [72] we used a different choice, where the subleading contribution reproduces the leading term in the second sum $\propto |Ha(t)\mathbf{x}|^{-\frac{3}{2}-\nu}$. We denote this by $\sigma_{pp}^{2(\mathrm{NLO})}$ and use it for comparison with Eq. (41c) in Sec. V. We discuss the differences this makes in the conclusions drawn in Ref. [72] in Appendix A. Henceforth, we will use Eq. (41) as our free noise but we include a more general formalism for calculating stochastic field correlators in Appendix B.

Since $\sigma_{qp}^{2(0)} = 0$, the variables p and q separate and so we now use two indices $(r, s) \in \{0, \infty\}$, corresponding to p and q, respectively, as opposed to just N. Thus, the free field eigenquations are given by

$$\mathcal{L}_{\mathrm{FP}}^{(0)}\Psi_{rs}^{(0)}(q,p) = -\Lambda_{rs}^{(0)}\Psi_{rs}^{(0)}(q,p), \tag{42a}$$

$$\mathcal{L}_{\mathrm{FP}}^{(0)*}\Psi_{rs}^{(0)*}(q,p) = -\Lambda_{rs}^{(0)}\Psi_{rs}^{(0)*}(q,p), \tag{42b}$$

where the $\Lambda_{rs}^{(0)}$ and $\Psi_{rs}^{(0)(*)}(q,p)$ are the free eigenvalues and (adjoint) eigenstates, respectively. The eigenvalues of Eq. (42) are

$$\Lambda_{rs}^{(0)} = (s\alpha + r\beta)H, \tag{43}$$

while the normalized eigenstates can be written in terms of the Hermite polynomials $H_n(x)$ as

$$\Psi_{rs}^{(0)}(q,p) = \frac{1}{\sqrt{2^{r+s}r!s!}}\left(\frac{\alpha\beta H^2}{\pi^2\sigma_{qq}^2\sigma_{pp}^2}\right)^{1/4} H_s\left(\sqrt{\frac{\alpha H}{\sigma_{qq}^2}}q\right) \times H_r\left(\sqrt{\frac{\beta H}{\sigma_{pp}^2}}p\right) e^{-\frac{\alpha H}{\sigma_{qq}^2}q^2-\frac{\beta H}{\sigma_{pp}^2}p^2}, \tag{44a}$$

$$\Psi_{rs}^{(0)*}(q,p) = \frac{1}{\sqrt{2^{r+s}r!s!}}\left(\frac{\alpha\beta H^2}{\pi^2\sigma_{qq}^2\sigma_{pp}^2}\right)^{1/4} H_s\left(\sqrt{\frac{\alpha H}{\sigma_{qq}^2}}q\right) \times H_r\left(\sqrt{\frac{\beta H}{\sigma_{pp}^2}}p\right). \tag{44b}$$

For the case where $\sigma_{pp}^2 = 0$, the eigenstates can be written as[1]

$$\lim_{\sigma_{pp}^2\to 0}\Psi_{rs}^{(0)}(q,\tilde{p}) = \frac{(-1)^{-r}}{\sqrt{2^{r+s}r!s!}}\left(\frac{\alpha H}{\sigma_{qq}^2}\right)^{1/4} \times \delta^{(r)}(\tilde{p})H_s\left(\sqrt{\frac{\alpha H}{\sigma_{qq}^2}}q\right)e^{-\frac{\alpha H}{\sigma_{qq}^2}q^2}, \tag{45a}$$

$$\lim_{\sigma_{pp}^2\to 0}\Psi_{rs}^{(0)*}(q,\tilde{p}) = \sqrt{\frac{2^r}{2^s r!s!}}\left(\frac{\alpha H}{\pi^2\sigma_{qq}^2}\right)^{1/4}\tilde{p}^r H_s\left(\sqrt{\frac{\alpha H}{\sigma_{qq}^2}}q\right), \tag{45b}$$

[1]To take the limit, we have used the identity $\lim_{\epsilon\to 0}\frac{(-1)^{-n}(\sqrt{2}\epsilon)^{n-1}}{\sqrt{\pi}}H_n(\frac{x}{\sqrt{2}\epsilon})e^{-\frac{x^2}{2\epsilon^2}} = \delta^{(n)}(x)$.

where $\tilde{p} = \sqrt{\frac{\beta H}{\sigma_{pp}^2}}p$ and the superscript (r) indicates that we are taking the rth derivative of the δ function. These are well-behaved eigenstates if we use $(q, \tilde{p})$ as our variables, with which we have the biorthogonality and completeness relations.

B. Stochastic perturbation theory

We will now move to the more interesting case of an interacting theory. To relate the stochastic correlators to the perturbative results of QFT, we expand our solutions to the eigenproblem (24) in terms of the (q, p) variables to $\mathcal{O}(\lambda)$,

$$\Lambda_{rs} = \Lambda_{rs}^{(0)} + \lambda\Lambda_{rs}^{(1)}, \tag{46a}$$

$$\Psi_{rs}^{(*)}(q,p) = \Psi_{rs}^{(0)(*)}(q,p) + \lambda\Psi_{rs}^{(1)(*)}(q,p). \tag{46b}$$

Using the eigenequations with the biorthogonality conditions for (q, p), equivalent to Eqs. (24) and (25), the $\mathcal{O}(\lambda)$ terms in the eigenvalues and eigenstates are given by

$$\Lambda_{rs}^{(1)} = -(\Psi_{rs}^{(0)*}, \mathcal{L}_{\mathrm{FP}}^{(1)}\Psi_{rs}^{(0)}), \tag{47a}$$

$$\Psi_{rs}^{(1)}(q,p) = \sum_{r's'}\Psi_{r's'}^{(0)}(q,p)\frac{(\Psi_{r's'}^{(0)*}, \mathcal{L}_{\mathrm{FP}}^{(1)}\Psi_{rs}^{(0)})}{\Lambda_{r's'}^{(0)} - \Lambda_{rs}^{(0)}}, \tag{47b}$$

$$\Psi_{rs}^{(1)*}(q,p) = \sum_{r's'}\Psi_{r's'}^{(0)*}(q,p)\frac{(\Psi_{r's'}^{(0)}, \mathcal{L}_{\mathrm{FP}}^{(1)*}\Psi_{rs}^{(0)*})}{\Lambda_{r's'}^{(0)} - \Lambda_{rs}^{(0)}}, \tag{47c}$$

where for Eqs. (47b) and (47c), $r' \neq r$ and $s' \neq s$. By applying the expansion (46) to Eq. (30), we can write the timelike correlator between two functions f and g to $\mathcal{O}(\lambda)$ as

$$\langle f(q_0,p_0)g(q,p)\rangle = \sum_{rs}\Big[f_{rs}^{(0)*}g_{rs}^{(0)} + \lambda(f_{rs}^{(0)*}g_{rs}^{(1)} + f_{rs}^{(1)*}g_{rs}^{(0)})\Big]e^{-(\Lambda_{rs}^{(0)}+\lambda\Lambda_{rs}^{(1)})t} \tag{48}$$

where $g_{rs} = g_{rs}^{(0)} + \lambda g_{rs}^{(1)}$ such that

$$g_{rs}^{(0)} = (\Psi_{rs}^{(0)}g, \Psi_{00}^{(0)*}), \tag{49a}$$

$$g_{rs}^{(1)} = (\Psi_{rs}^{(1)}g, \Psi_{00}^{(0)*}) + (\Psi_{rs}^{(0)}g, \Psi_{00}^{(1)*}) \tag{49b}$$

with a similar relation holding for f_{rs}^*. A similar expression for the spacelike correlator can be written using Eq. (34) as

$$\begin{aligned}\langle f(q_1,p_1)g(q_2,p_2)\rangle = \int dq_r \int dp_r \sum_{r'rs's} \Bigg[& \frac{\Psi_{00}^{(0)}(q_r,p_r)}{\Psi_{00}^{(0)*}(q_r,p_r)} \Psi_{rs}^{(0)*}(q_r,p_r)\Psi_{r's'}^{(0)*}(q_r,p_r) f_{rs}^{(0)} g_{r's'}^{(0)} \\ & + \lambda \Bigg(\frac{\Psi_{00}^{(1)}(q_r,p_r)}{\Psi_{00}^{(0)*}(q_r,p_r)} \Psi_{rs}^{(0)*}(q_r,p_r)\Psi_{r's'}^{(0)*}(q_r,p_r) f_{rs}^{(0)} g_{r's'}^{(0)} \\ & - \frac{\Psi_{00}^{(1)*}(q_r,p_r)\Psi_{00}^{(0)}(q_r,p_r)}{\Psi_{00}^{(0)*}(q_r,p_r)^2} \Psi_{rs}^{(0)*}(q_r,p_r)\Psi_{r's'}^{(0)*}(q_r,p_r) f_{rs}^{(0)} g_{r's'}^{(0)} \\ & + \frac{\Psi_{00}^{(0)}(q_r,p_r)}{\Psi_{00}^{(0)*}(q_r,p_r)} \Psi_{rs}^{(1)*}(q_r,p_r)\Psi_{r's'}^{(0)*}(q_r,p_r) f_{rs}^{(0)} g_{r's'}^{(0)} + \frac{\Psi_{00}^{(0)}(q_r,p_r)}{\Psi_{00}^{(0)*}(q_r,p_r)} \Psi_{rs}^{(0)*}(q_r,p_r)\Psi_{r's'}^{(1)*}(q_r,p_r) f_{rs}^{(0)} g_{r's'}^{(0)} \\ & + \frac{\Psi_{00}^{(0)}(q_r,p_r)}{\Psi_{00}^{(0)*}(q_r,p_r)} \Psi_{rs}^{(0)*}(q_r,p_r)\Psi_{r's'}^{(0)*}(q_r,p_r) f_{rs}^{(1)} g_{r's'}^{(0)} \\ & + \frac{\Psi_{00}^{(0)}(q_r,p_r)}{\Psi_{00}^{(0)*}(q_r,p_r)} \Psi_{rs}^{(0)*}(q_r,p_r)\Psi_{r's'}^{(0)*}(q_r,p_r) f_{rs}^{(0)} g_{r's'}^{(1)} \Bigg) \Bigg] |Ha(t)(\mathbf{x}_1-\mathbf{x}_2)|^{-\left(\frac{\Lambda_{rs}^{(0)}+\Lambda_{r's'}^{(0)}}{H}+\lambda\frac{\Lambda_{rs}^{(1)}+\Lambda_{r's'}^{(1)}}{H}\right)}. \end{aligned} \tag{50}$$

In this paper we focus on the spacelike correlator.

We are now in a position where we can substitute explicit expressions for the eigenvalues and eigenstates in terms of the noise amplitudes (41). We will only consider the zeroth and first two nonzero states in the spectral expansion since these are the only terms that are needed to compare stochastic and QFT results. Hence, we only need to concern ourselves with finding the terms in the correlators corresponding to (r,s) equal to $(0,0)$, $(0,1)$, and $(1,0)$. From Eq. (47), the $\mathcal{O}(\lambda)$ corrections to the first two eigenvalues are

$$\Lambda_{00}^{(1)} = 0, \tag{51a}$$

$$\Lambda_{01}^{(1)} = \frac{3H\Gamma(\nu)\Gamma(\frac{3}{2}-\nu)}{8\pi^{5/2}\nu}, \tag{51b}$$

where the fact that $\Lambda_{00}^{(1)} = 0$ is consistent with its correspondence to the equilibrium solution. Using Eq. (50), we can find the spacelike $q-q$, $q-p$, $p-q$, and $p-p$ stochastic correlators. To complete our perturbative expansion, we also need to account for the λ dependence in the noise by

$$\sigma_{ij}^2 = \sigma_{ij}^{2(0)} + \lambda\sigma_{ij}^{2(1)}. \tag{52}$$

Note that we will show to relative order $\mathcal{O}(\frac{\lambda H^4}{m^4})$ that $\sigma_{ij}^{2(1)}$ is zero; however, at this stage it is important to show that no such IR-divergent piece contributes. To $\mathcal{O}(\lambda)$, the spacelike (q,p) stochastic correlators are

$$\langle q(t,\mathbf{0})q(t,\mathbf{x})\rangle = \left[\frac{H^4\Gamma(1+\nu)\Gamma(\frac{5}{2}-\nu)}{2\pi^{5/2}m^2} + \lambda\left(\frac{\sigma_{qq}^{2(1)}}{H(3-2\nu)} - \frac{3H^4\Gamma(\nu)^2\Gamma(\frac{3}{2}-\nu)^2}{8\pi^5(3+2\nu)m^2}\right)\right]|Ha(t)\mathbf{x}|^{-\frac{2\Lambda_{01}}{H}}, \tag{53a}$$

$$\langle q(t,\mathbf{0})p(t,\mathbf{x})\rangle = \langle p(t,\mathbf{0})q(t,\mathbf{x})\rangle = -\frac{3\lambda H^3\Gamma(\nu)^2\Gamma(\frac{3}{2}-\nu)^2}{32\pi^5\nu}|Ha(t)\mathbf{x}|^{-\frac{2\Lambda_{01}}{H}} + \lambda\left(\frac{\sigma_{qp}^{2(1)}}{3H} + \frac{H^5\Gamma(\nu)^2\Gamma(\frac{5}{2}-\nu)^2}{16\pi^5\nu m^2}\right)|Ha(t)\mathbf{x}|^{-3}, \tag{53b}$$

$$\langle p(t,\mathbf{0})p(t,\mathbf{x})\rangle = \frac{\lambda\sigma_{pp}^{2(1)}}{H(3+2\nu)}|Ha(t)\mathbf{x}|^{-\frac{2\Lambda_{10}}{H}}. \tag{53c}$$

Substituting these expressions into Eq. (40), we obtain an expression for the $\phi-\phi$ stochastic correlator up to first order in λ. The spacelike version is

$$\langle\phi(t,\mathbf{0})\phi(t,\mathbf{x})\rangle = \left[\frac{H^2}{16\pi^2}\frac{\Gamma(\frac{3}{2}-\nu)\Gamma(2\nu)4^{\frac{3}{2}-\nu}}{\Gamma(\frac{1}{2}+\nu)} + \lambda\left(\frac{(3+2\nu)\sigma_{qq}^{2(1)}}{4\nu H(3-2\nu)} + \frac{3(3-4\nu)H^4\Gamma(\nu)^2\Gamma(\frac{3}{2}-\nu)^2}{32\pi^5\nu m^2}\right)\right]|Ha(t)\mathbf{x}|^{-\frac{2\Lambda_{01}}{H}} + \frac{\lambda\sigma_{pp}^{2(1)}}{H^3\nu(3+2\nu)^2}|Ha(t)\mathbf{x}|^{-\frac{2\Lambda_{10}}{H}} - \lambda\left(\frac{\sigma_{qp}^{2(1)}}{3H^2\nu} + \frac{H^4\Gamma(\nu)^2\Gamma(\frac{5}{2}-\nu)^2}{8\pi^5\nu m^2}\right)|Ha(t)\mathbf{x}|^{-3}. \tag{54}$$

C. Second-order stochastic parameters

In Sec. II we found the Feynman propagator to $\mathcal{O}(\lambda)$. We will use this result to match the $\mathcal{O}(\lambda)$ noise. First, we need to match the stochastic mass m to the parameters m_R and λ from the QFT such that the exponents of Eqs. (10) and (54) agree to relative order $\mathcal{O}(\frac{\lambda H^4}{m^4})$. Combining the free and interacting parts of the first nonzero eigenvalue, we find that to relative order $\mathcal{O}(\frac{\lambda H^4}{m^4})$

$$\Lambda_{01} = \left(\frac{3}{2}-\nu\right)H + \frac{3\lambda H^3}{8\pi^2 m^2} + \mathcal{O}(\lambda H) \tag{55}$$

has the same functional form as the exponent in the Feynman propagator (11). This tells us that the stochastic mass $m^2 = m_R^2(1+\mathcal{O}(\frac{\lambda H^2}{m_R^2}))$. In particular, they agree at relative order $\mathcal{O}(\frac{\lambda H^4}{m^4})$ and thus the stochastic exponent can be found for $\lambda \ll m^2/H^2$, in contrast to the direct perturbative calculation which requires $\lambda \ll m^4/H^4$. In order to compute the term at relative order $\mathcal{O}(\frac{\lambda H^2}{m_R^2})$, we would have to choose a regularization scheme. This will be considered in future work [73]. For the rest of this paper, we will just set any $\mathcal{O}(\frac{\lambda H^2}{m^2})$ corrections—be they quantum or stochastic—to zero. It is noteworthy that Eq. (55) is also obtained if we were to choose $\sigma_{pp}^2 = \sigma_{pp}^{2(\mathrm{NLO})}$.

To match the amplitude, we expand the spacelike stochastic field correlator (54) to relative order $\mathcal{O}(\frac{\lambda H^4}{m^4})$, resulting in

$$\langle\phi(t,\mathbf{0})\phi(t,\mathbf{x})\rangle = \left[\frac{3H^4}{8\pi^2m^2} - \frac{27\lambda H^8}{64\pi^4m^6} + \frac{3H\sigma_{qq}^{2(1)}}{2m^2} + \mathcal{O}\left(\frac{\lambda H^6}{m^4}\right)\right]|Ha(t)\mathbf{x}|^{-\frac{2m^2}{3H^2}+\frac{3\lambda H^2}{4\pi^2m^2}+\mathcal{O}(\lambda)} + \left(\frac{\lambda\sigma_{pp}^{2(1)}}{54H^3} + \mathcal{O}\left(\frac{\lambda H^4}{m^2}\right)\right)|Ha(t)\mathbf{x}|^{-3-\frac{2m^2}{3H^2}-\frac{3\lambda H^2}{4\pi^2m^2}+\mathcal{O}(\lambda)} + \lambda\left(\frac{2\sigma_{qp}^{2(1)}}{9H^2} + \mathcal{O}\left(\frac{\lambda H^4}{m^2}\right)\right)|Ha(t)\mathbf{x}|^{-3}. \tag{56}$$

We see that if we set all three $\mathcal{O}(\lambda)$ noise amplitudes to zero, we reproduce the Feynman propagator to relative order $\mathcal{O}(\frac{\lambda H^4}{m^4})$. Thus, our matched noise from perturbation theory is

$$\sigma_{qq}^2 = \frac{2H^3\Gamma(1+\nu)\Gamma(\frac{5}{2}-\nu)}{\pi^{5/2}(3+2\nu)} + \mathcal{O}\left(\frac{\lambda H^5}{m^2}\right), \tag{57a}$$

$$\sigma_{qp}^2 = 0 + \mathcal{O}\left(\frac{\lambda H^6}{m^2}\right), \tag{57b}$$

$$\sigma_{pp}^2 = 0 + \mathcal{O}\left(\frac{\lambda H^7}{m^2}\right). \tag{57c}$$

We are assuming that $\sigma_{qp}^{2(0)}$ and $\sigma_{pp}^{2(0)}$ are parametrically $\mathcal{O}(H^4)$ and $\mathcal{O}(H^5)$, respectively, such that the correction to all three noise amplitudes is of the same relative order $\mathcal{O}(\frac{\lambda H^2}{m^2})$. Converting the noise amplitudes to (ϕ,π) variables gives

$$\sigma^2 = \frac{H^3\Gamma(\nu)\Gamma(\frac{5}{2}-\nu)}{2\pi^{5/2}} \times \begin{pmatrix} 1+\mathcal{O}(\frac{\lambda H^5}{m^2}) & -\frac{2m^2}{H(3+2\nu)}+\mathcal{O}(\frac{\lambda H^6}{m^2}) \\ -\frac{2m^2}{H(3+2\nu)}+\mathcal{O}(\frac{\lambda H^6}{m^2}) & \frac{4m^4}{(3+2\nu)^2H^2}+\mathcal{O}(\frac{\lambda H^7}{m^2}) \end{pmatrix}. \tag{58}$$

This matrix gives the components of the noise aligning with Eq. (18).

D. Comparing models and their limitations

The strength of a stochastic approach is that the Fokker-Planck equation can be solved—analytically for some examples, but usually numerically—and therefore correlation functions can be obtained nonperturbatively. The second-order stochastic approach loses some of this power because it requires the noise to be calculated perturbatively and therefore we are at present limited to the regime $\frac{\lambda H^2}{m^2} \ll 1$. To investigate the usefulness of this approach, we compare its regime of validity with that of the other two approximations introduced above: perturbative QFT and stochastic OD. Their respective regimes of validity are

$$\text{Perturbative QFT}: \lambda \ll \frac{m^4}{H^4}, \quad \lambda \ll 1, \tag{59a}$$

$$\text{OD stochastic}: \lambda \ll \frac{m^2}{H^2}, \quad m \ll H, \tag{59b}$$

$$\text{Second-order stochastic}: \lambda \ll \frac{m^2}{H^2}, \quad m \lesssim H. \tag{59c}$$

A comparison between these regimes is given in Fig. 1. For the purposes of making the boundaries obvious, we choose "≪ 1" to mean "< 0.2" in this plot. In reality, we would not expect these boundaries to be so clear cut.

Perturbative QFT is encompassed by the second-order stochastic approach in the limit $m \lesssim H$, which is unsurprising given that the matched correlators were found directly from the Feynman propagators. The OD results should also be completely covered by the second-order stochastic approach (we will confirm this in Sec. V B 3) and are resigned to the left-hand side of Fig. 1 as the approximation requires the fields to be light. Importantly, this leaves an area in the parameter space—the purely orange zone—where we expect the second-order stochastic approach to work when the others do not. To obtain such results, we need to numerically solve our two-dimensional Fokker-Planck equation. From this, we can compare the three approximations.

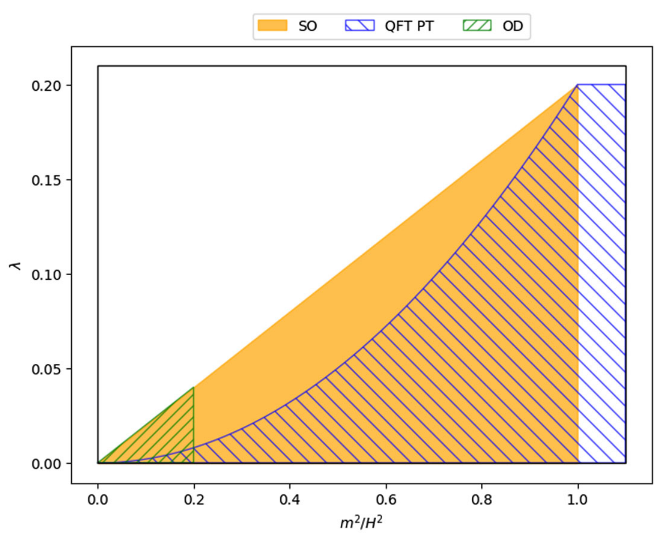

FIG. 1. Regimes in which we expect our approximations to work. Perturbative QFT, OD stochastic, and second-order (SO) stochastic are expected to work in the blue left-hashed, green right-hashed, and orange regions, respectively. Note that there is some overlap. The pure white space is where none of these approximations work.

V. NUMERICAL SOLUTIONS TO THE FOKKER-PLANCK EQUATION

A. Expansion in free eigenstates

Thus far, we have shown that the second-order stochastic approach can be made to coincide with perturbative QFT if we choose the stochastic parameters to be Eq. (57). We will now solve the stochastic equations numerically to obtain nonperturbative results. We continue to use the (q, p) coordinates so that we can continue to use the free eigenstates (44). We make the ansatz that our eigensolutions to the eigenequations (24) can be written as

$$\Psi_N(q,p) = \sum_{rs} c_{rs}^{(N)} \psi_{rs}^{(0)}(q,p), \tag{60a}$$

$$\Psi_N^*(q,p) = \sum_{rs} c_{rs}^{*(N)} \psi_{rs}^{(0)*}(q,p), \tag{60b}$$

where $c_{rs}^{(*)(N)}$ are two sets of coefficients to be determined and $\psi_{rs}^{(0)*}(q,p)$ are the free eigenstates given in Eq. (44). Substituting Eq. (60) into Eq. (24) gives

$$\sum_{rs} c_{rs}^{(N)} \mathcal{L}_{\mathrm{FP}} \psi_{rs}^{(0)}(q,p) = -\Lambda_N \sum_{rs} c_{rs}^{(N)} \psi_{rs}^{(0)}(q,p), \tag{61a}$$

$$\sum_{rs} c_{rs}^{(N)} \mathcal{L}_{\mathrm{FP}}^* \psi_{rs}^{(0)*}(q,p) = -\Lambda_N \sum_{rs} c_{rs}^{*(N)} \psi_{rs}^{(0)*}(q,p). \tag{61b}$$

Applying the Fokker-Planck operator to the free eigenstates will give us

$$\mathcal{L}_{\mathrm{FP}}^{(*)} \psi_{rs}^{(0)(*)}(q,p) = \sum_{r's'} \mathcal{M}_{rsr's'}^{(*)} \psi_{r's'}^{(0)(*)}, \tag{62}$$

where the matrices $\mathcal{M}^{(*)}$ are given by

$$\mathcal{M}_{rsr's'} = (\psi_{r's'}^{(0)*}, \mathcal{L}_{\mathrm{FP}} \psi_{rs}^{(0)}) = \mathcal{M}_{r's'rs}^*. \tag{63}$$

Explicit expressions for these matrices can be found but they are complicated. Applying Eq. (62) to Eq. (61) and making use of the completeness of the free eigenstates (25), one can write

$$\sum_{r's'} \mathcal{M}_{rsr's'}^T c_{r's'}^{(N)} = -\Lambda_N c_{rs}^{(N)}, \tag{64a}$$

$$\sum_{r's'} (\mathcal{M}^*)_{rsr's'}^T c_{r's'}^{*(N)} = -\Lambda_N c_{rs}^{*(N)}. \tag{64b}$$

Thus, by diagonalizing the matrices $(\mathcal{M}^{(*)})^T$, we can obtain the eigenvalues Λ_N and the coefficients $c_{rs}^{*(N)}$ and hence the full solution to the Fokker-Planck equation.

In theory, this sum is infinite and our matrices are infinite dimensional. Therefore, we have to choose values for r and s ($r_{\max}$ and $s_{\max}$, respectively) at which we truncate the series so that we can practically diagonalize the matrices. This approximation only works if the expansion in our chosen eigenstates (60) converges as $r_{\max}$ and $s_{\max}$ become large. Indeed, we can use this fact to improve the accuracy of the spectral expansion by evaluating the eigenvalues for a range of r and s and then fitting an appropriate curve that converges at infinity. This essentially gives us the eigenvalue at infinity. There will naturally be some error associated with this fit but, as we will see, it is exceedingly small. The convergence speeds up as m^2/H^2 increases with constant λ and as λ decreases with constant m^2/H^2. This is the case where the free solution is the dominant one.

For the purposes of this work, we focus on calculating the first nonzero eigenvalue in our spectral expansion Λ_1. To make the idea of truncation and fitting more concrete, we consider the specific example in Fig. 2 where we calculate Λ_1 at $m^2/H^2 = 0.01$ and $\lambda = 0.0005$ with the level of truncation $(r_{\max}, s_{\max})$ ranging from (26, 26) to (34, 34). The fit in Fig. 2 gives the eigenvalue at infinity $\Lambda_1^{(\infty)} = 0.004530997449(4)$. The error is exceedingly small, of order 10^{-12}. Even if one just studies Fig. 2 roughly, one can see that the value of Λ_1 changes on the scale of 10^{-10} when going from a truncation at (26, 26) to (34, 34), 7 orders of magnitude below the leading significant figure of the eigenvalue. This is so small that we can consider our numerical approach to have negligible error. This is the scale of errors for all data taken in this work and therefore we can ignore numerical errors and henceforth drop the superscript (∞).

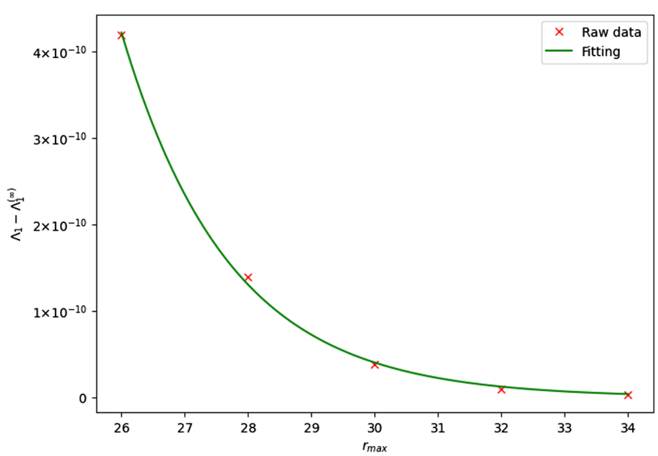

FIG. 2. Difference between the first nonzero eigenvalue as found at the highest order of truncation Λ_1 and the fit $\Lambda_1^{(\infty)} = 0.004530997449(4)$ for a range of $(r_{\max}, s_{\max})$ at $m^2/H^2 = 0.01$ and $\lambda = 0.0005$. Red crosses are the data found by numerically diagonalizing the matrix $\mathcal{M}^T$ up to the truncation $(r_{\max}, s_{\max})$ and the green line is the fit, which is exponential. Note that we always take $r_{\max} = s_{\max}$ and hence use a single number, $r_{\max}$, to label the x axis.

B. Comparing the second-order stochastic approach to the OD limit and perturbative QFT

We now have a nonperturbative approach for finding the eigenvalues associated with the second-order Fokker-Planck equation (19). The only perturbative effect in these eigenvalues is in the relationship between the parameters of the second-order stochastic approach and QFT. Thus, we have the spectrum of solutions that covers the region $\frac{\lambda H^2}{m^2} \ll 1$ in the parameter space (the orange region in Fig. 1). This encompasses the parameter space where the OD approximation is valid. However, thus far we have not explicitly checked that the OD and second-order results agree. To do this, we calculate the first nonzero eigenvalue in each method in the region where the OD approach is valid, $m^2/H^2 \ll 1$ and $\lambda \ll m^2/H^2$.

We also make an explicit comparison with the perturbative QFT eigenvalue (11). This is done to check that the eigenvalues of the second-order stochastic approach behave as expected; there should be a good level of agreement in the regimes where the established approximations are valid and a degree of difference when they are not.

1. Example 1: $m^2/H^2 = 0.1$

We start by considering two examples of how Λ_1 compares to the equivalent quantities in the other two approximations by plotting them as a function of λ for constant m^2/H^2. For clarity, we label the first nonzero state of the second-order stochastic approach as $\Lambda_1^{(SO)}$. In both Figs. 3 and 4, the solid cyan line shows the choice $\sigma_{pp}^2 = 0$ (57c) with the choice $\sigma_{pp}^{2(\mathrm{NLO})}$ [Eq. (59c) of Ref. [72]] shown for comparison as the dot-dashed cyan line. One can see that in both figures the two cyan lines diverge from one another as λ increases, suggesting that the choice of σ_{pp}^2 is important. This is not the case. The reason for the discrepancy is because we have not included the one-loop corrections to the stochastic parameters, which enter at relative order $\frac{\lambda H^2}{m^2}$, so this difference really tells us the size of such corrections. If one were to include these, the choice of σ_{pp}^2 would be irrelevant. This will be undertaken in future work [73].

The first example is for $m^2/H^2 = 0.1$. This is chosen because the mass is sufficiently small such that the OD stochastic approach will be valid beyond both the perturbative QFT and second-order stochastic approaches. Consider Fig. 3. One can see that for small λ, all three

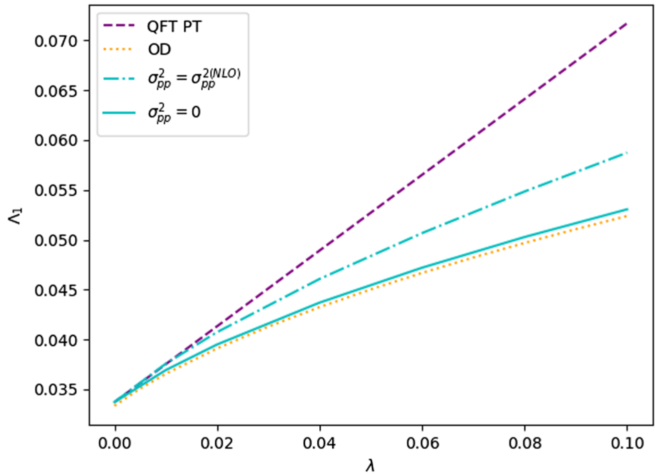

FIG. 3. Plot of the first excited eigenvalue Λ_1 as a function of λ for $m^2/H^2 = 0.1$ using the perturbative QFT (purple, dashed), OD stochastic (orange, dotted), and second-order stochastic (cyan) approaches, with $\sigma^2_{pp} = \sigma^{2(\mathrm{NLO})}_{pp}$ (dot-dashed) and $\sigma^2_{pp} = 0$ (solid).

models converge. This is as expected because it is in this limit that all three models are valid. As we move towards higher λ, $\frac{\lambda H^4}{m^4}$ quickly becomes comparable to 1 and therefore the perturbative QFT eigenvalue diverges from the other three curves. This divergence is large, which is no surprise because even at $\lambda = 0.01$, $\frac{\lambda H^4}{m^4} = 1$ so we are already out of the regime of validity for perturbative QFT. One can see that there is good agreement between the OD and second-order stochastic approaches throughout for $\sigma^2_{pp} = 0$, as expected, as we are still in the region where the two models should agree.

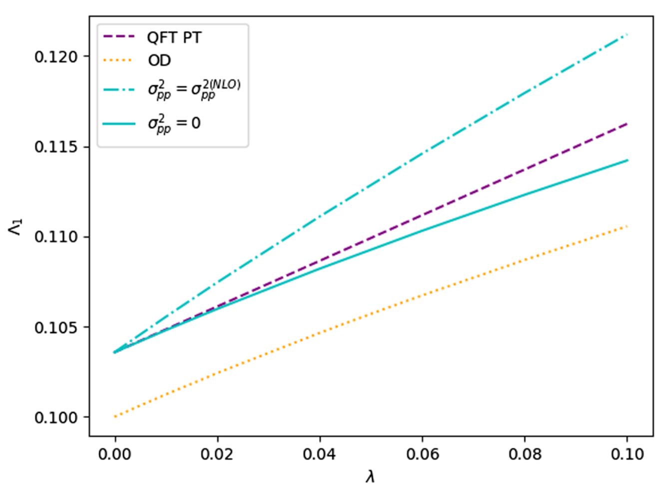

FIG. 4. Plot of the first excited eigenvalue Λ_1 as a function of λ for $m^2/H^2 = 0.3$ using the perturbative QFT (purple, dashed), OD stochastic (orange, dotted), and second-order stochastic (cyan) approaches, with $\sigma^2_{pp} = \sigma^{2(\mathrm{NLO})}_{pp}$ (dot-dashed) and $\sigma^2_{pp} = 0$ (solid).

2. Example 2: $m^2/H^2 = 0.3$

For our second example, we consider a larger mass $m^2/H^2 = 0.3$ such that the OD stochastic results become less reliable. Consider Fig. 4. One can see that for small λ the second-order stochastic and perturbative QFT results agree well, but as one increases λ the two results diverge from each other. This is once again because increasing λ results in an increase of $\frac{\lambda H^4}{m^4}$. Conversely, even at small λ, the OD stochastic approach gives a different value for the eigenvalue compared to the other two approaches, suggesting that even at $m^2/H^2 = 0.3$ we are at too high a mass for the OD stochastic approach to be trustworthy.

3. OD versus second-order stochastic approaches

From these two examples, we can see that the behavior of the second-order stochastic approach is as expected; there is agreement and difference in the regimes where one would expect to find them. To make this more quantitative, we now consider more carefully the difference between eigenvalues between the second-order stochastic approach and the other two approaches.

First, we consider the difference between the second-order and OD stochastic results. We take the relative difference between the second-order and OD eigenvalues $\frac{\Lambda_1^{(\mathrm{SO})} - \Lambda_1^{(\mathrm{OD})}}{\Lambda_1^{(\mathrm{SO})}}$ as a function of m^2/H^2. As one increases m^2/H^2 the OD stochastic approach becomes less reliable so we expect to see an increase in the difference between the two results. In Fig. 5 we plot the relative difference for different values of λ for the case when $\sigma^2_{pp} = 0$. We immediately see that all of the curves follow the same linearly increasing behavior. As we increase m^2/H^2 towards the right-hand side of the figure, we see that the relative difference increases, as expected.

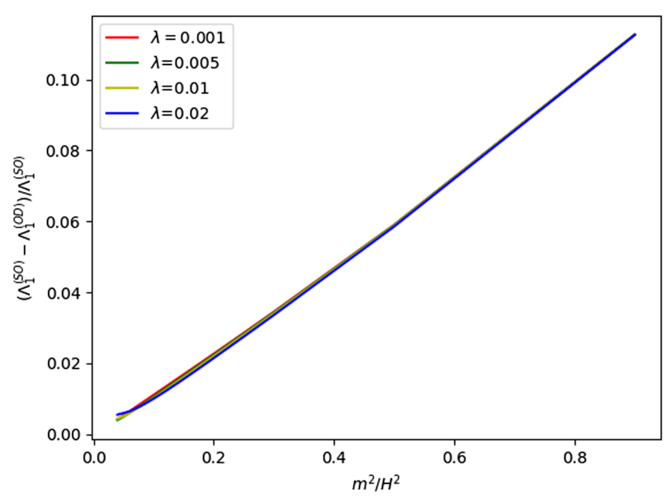

FIG. 5. Plot of $\frac{\Lambda_1^{(\mathrm{SO})} - \Lambda_1^{(\mathrm{OD})}}{\Lambda_1^{(\mathrm{SO})}}$ against m^2/H^2 for $\lambda = 0.001$ (red), 0.005 (green), 0.01 (yellow), and 0.02 (blue).

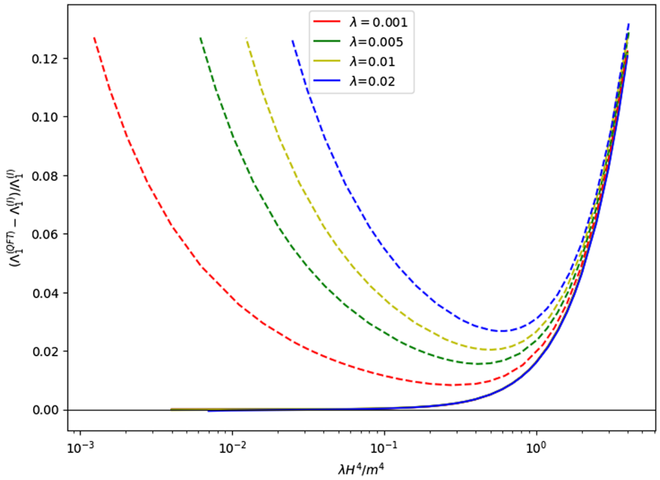

FIG. 6. Plot of $\frac{\Lambda_1^{(\mathrm{QFT})}-\Lambda_1^{(I)}}{\Lambda_1^{(I)}}$, where $I\in\{\mathrm{SO},\mathrm{OD}\}$ as a function of $\frac{\lambda H^4}{m^4}$ for $\lambda=0.001$ (red), $\lambda=0.005$ (green), $\lambda=0.01$ (yellow), and $\lambda=0.02$ (blue). The solid lines show the relative difference between the SO and QFT eigenvalues, which lie directly on top of each other for most $\frac{\lambda H^4}{m^4}$ values, while the dashed lines show the relative difference between the OD and QFT eigenvalues.

4. *Perturbative QFT versus second-order stochastic approaches*

We now do the same analysis with a comparison of the second-order stochastic and perturbative QFT eigenvalues where we plot the eigenvalue difference $\frac{\Lambda_1^{(\mathrm{QFT})}-\Lambda_1^{(\mathrm{SO})}}{\Lambda_1^{(\mathrm{SO})}}$ for several values of λ (solid lines in Fig. 6). Now, we use $\lambda H^4/m^4$ on the x axis. As one increases this parameter, perturbative QFT becomes less reliable so we expect to see an increase in the difference between the two results. We see the expected behavior: for small $\frac{\lambda H^4}{m^4}$, all of the curves converge to 0. As $\frac{\lambda H^4}{m^4}$ increases, we see an increasing relative difference between the two eigenvalues due to a breakdown of perturbative QFT.

5. *OD stochastic versus perturbative QFT approaches*

The final comparison we make is between the two established approximations: perturbative QFT and the OD stochastic approach. The dotted lines in Fig. 6 plot the eigenvalue difference between the two approaches, $\frac{\Lambda_1^{(\mathrm{QFT})}-\Lambda_1^{(\mathrm{OD})}}{\Lambda_1^{(\mathrm{OD})}}$, as a function of $\frac{\lambda H^4}{m^4}$ for the four λ values.

On the right-hand side of the plot, we can see that the deviation from the QFT result follows the same pattern as that of the second-order stochastic approach. This is unsurprising because, as we move to higher $\frac{\lambda H^4}{m^4}$, we are moving to smaller m^2/H^2, the limit where the OD and second-order stochastic approaches agree. In this regime, perturbative QFT is breaking down so we see a high relative difference between it and the stochastic approaches. As we move to smaller values of $\frac{\lambda H^4}{m^4}$, the dotted curves dip to some minimum before turning upward. As one moves left, there is an increasing relative difference between the two; this is now due to the breakdown of the OD stochastic approach since we are getting to high m^2/H^2 values. One can see that the second-order stochastic approach continues towards a zero relative difference, indicating the region where the OD approach breaks down but the other two approximations are still valid.

VI. CONCLUDING REMARKS

We have shown that the second-order stochastic effective theory can be used to calculate correlation functions for self-interacting scalar fields in de Sitter spacetime. The stochastic parameters were determined by matching stochastic correlators to their counterparts in perturbative QFT and a novel numerical calculation was implemented in order to perform computations for fields of mass $m\lesssim H$ and coupling $\lambda\ll m^2/H^2$. This goes beyond the regimes of the established approximations of perturbative QFT and the overdamped stochastic approach, which are limited to $\lambda\ll m^4/H^4$ and $m\ll H$, $\lambda\ll m^2/H^2$, respectively. It would be interesting to compare our results to other nonperturbative approaches, but that is beyond the scope of this paper.

Future work is in progress to extend the second-order stochastic approach further to incorporate the full one-loop correction, which will capture the relative order $\mathcal{O}(\frac{\lambda H^2}{m^2})$ contributions. This will improve the results of the current paper and extend the regime of validity of the second-order stochastic theory even further. Ideally, one would like to derive the stochastic parameters from an underlying quantum theory nonperturbatively as opposed to using the perturbative matching procedure; however, it is not clear how one should proceed in this direction.

Regardless, the second-order stochastic effective theory has strong computational power that will be useful in a range of topics in inflationary cosmology, such as the precision calculation of the primordial curvature and isocurvature perturbations in scenarios with light scalar fields. The formalism outlined in this work suggests that the stochastic approach has applications beyond its widely used overdamped state and that it is a method that warrants further study.

ACKNOWLEDGMENTS

A. C. was supported by a UK Science and Technology Facility Council studentship. A. R. was supported by Science Technology and Facility Council (STFC) Grants ST/P000762/1 and ST/T000791/1 and an Institute for Particle Physics Phenomenology (IPPP) Associateship. A. C. would like to thank Anders Tranberg and Magdalena Eriksson for useful discussions. We would also like to thank Grigoris Pavliotis for his insight.

APPENDIX A: CHOICE OF THE *pp* NOISE AMPLITUDE

The choice of setting $\sigma^2_{pp} = 0$ as opposed to fitting it with the subleading contribution is a deviation from our work in Ref. [72] and so it is worth discussing here where any difference may occur. The key difference we need to address here is the comparison we made in Eq. (71) of Ref. [72]. In that work, we had an alternative second-order stochastic approach, where one introduced a cutoff between the sub- and superhorizon modes. We compared this with the matching procedure for free fields and showed that the two models would only reproduce equivalent leading-order contributions in the limit $m \ll H$. Here, we show these results again for free fields but also include the matching prescription when $\sigma^2_{pp} = 0$ as well. The result is

$$\sigma^{2(0)}_{qq}\Big|_{m\ll H} = \frac{H^3}{4\pi^2},\qquad \sigma^2_{\mathrm{cut},qq}\Big|_{m\ll H} = \frac{H^3}{4\pi^2}\left(1+\frac{\epsilon^2}{3}+\frac{\epsilon^4}{9}\right); \tag{A1a}$$

$$\sigma^{2(0)}_{qp}\Big|_{m\ll H} = 0,\qquad \sigma^2_{\mathrm{cut},qp}\Big|_{m\ll H} = \frac{H^4}{4\pi^2}\left(-\epsilon^2+\frac{\epsilon^4}{3}\right); \tag{A1b}$$

$$\sigma^{2(0)}_{pp}\Big|_{m\ll H} = \begin{cases}\sigma^{2(\mathrm{NLO})}_{pp}|_{m\ll H} = \frac{36H^5}{\pi^2},\\ 0,\end{cases}\qquad \sigma^2_{\mathrm{cut},pp}|_{m\ll H} = \frac{H^5}{4\pi^2}\epsilon^4. \tag{A1c}$$

ϵ is the cutoff parameter which one takes to be small such that $\epsilon^2 \sim 0$. We see that the two approaches agree for all three noise amplitudes if $\sigma^{2(0)}_{pp} = 0$. This is not what is found if one matches σ^2_{pp} with the subleading contribution, when $\sigma^{2(0)}_{pp} = \sigma^{2(\mathrm{NLO})}_{pp}$.

This choice also proves convenient because it is now straightforward to recover the OD stochastic equations from the full second-order theory. Writing the (ϕ, π) noise amplitudes found through matching in the limit $m \ll H$,

$$\sigma^2_{\phi\phi}|_{m\ll H} = \frac{H^3}{4\pi^2}, \tag{A2a}$$

$$\sigma^2_{\phi\pi}|_{m\ll H} = 0, \tag{A2b}$$

$$\sigma^2_{\pi\pi}|_{m\ll H} = 0, \tag{A2c}$$

we see that the only nonzero component to the noise amplitude is $\sigma^2_{\phi\phi}$. Considering Eq. (16) in the OD limit $\dot{\pi} \ll 3H\pi$, it becomes

$$\dot{\phi} + \frac{V'(\phi)}{3H} = \xi_\phi, \tag{A3}$$

which is just the OD stochastic equation (12).

APPENDIX B: STOCHASTIC PERTURBATION THEORY USING GENERAL NOISE

In this appendix, we outline the derivation of the stochastic field correlator for a general noise contribution. We include both the timelike and spacelike correlators for completeness.

From Eq. (47), the lowest two eigenvalues at $\mathcal{O}(\lambda)$ are

$$\Lambda^{(1)}_{00} = 0, \tag{B1a}$$

$$\Lambda^{(1)}_{01} = \frac{3\alpha\sigma^2_{pp} - 4H\alpha\beta^2\sigma^2_{qp} + 3H^2\beta^3\sigma^2_{qq}}{8\nu^2H^4\alpha\beta^2}. \tag{B1b}$$

By using Eqs. (48) and (50), respectively, we can find the timelike and spacelike $q-q$, $q-p$, $p-q$, and $p-p$ stochastic correlators. Including the perturbed noise (52), the timelike (q, p) stochastic correlators to $\mathcal{O}(\lambda)$ are

$$\begin{aligned}\langle q(0,\mathbf{x})q(t,\mathbf{x})\rangle = {}& \left[\frac{\sigma^{2(0)}_{qq}}{2H\alpha} + \lambda\left(\frac{\sigma^{2(1)}_{qq}}{2H\alpha} + \frac{(3\nu H\sigma^{2(0)}_{qq} - \alpha\sigma^{2(0)}_{qp})(3\alpha\sigma^{2(0)}_{pp} - 4H\alpha\beta^2\sigma^{2(0)}_{qp} + 3H^2\beta^3\sigma^{2(0)}_{qq})}{48\nu^3H^7\alpha^3\beta^2}\right)\right]\\ &\times e^{-\left(\alpha H + \lambda\frac{3\alpha\sigma^{2(0)}_{pp} - 4H\alpha\beta^2\sigma^{2(0)}_{qp} + 3H^2\beta^3\sigma^{2(0)}_{qq}}{8\nu^2H^4\alpha\beta^2}\right)t}\\ &+ \left[\lambda\left(\frac{\sigma^{2(0)}_{qp}(-3\alpha\sigma^{2(0)}_{pp} + 4H\alpha\beta^2\sigma^{2(0)}_{qp} - 3H^2\beta^3\sigma^{2(0)}_{qq})}{48\nu^3H^7\alpha\beta^3}\right)\right] e^{-\left(\beta H - \lambda\frac{3\alpha\sigma^{2(0)}_{pp} - 4H\alpha\beta^2\sigma^{2(0)}_{qp} + 3H^2\beta^3\sigma^{2(0)}_{qq}}{8\nu^2H^4\alpha\beta^2}\right)t},\end{aligned} \tag{B2a}$$

$$\langle p(0,\mathbf{x})q(t,\mathbf{x})\rangle = \left[\frac{\sigma_{qp}^{2(0)}}{3H} + \lambda\left(\frac{\sigma_{qp}^{2(1)}}{3H} + \frac{(\nu H^2\beta^2\sigma_{qq}^{2(0)} - \alpha\sigma_{pp}^{2(0)})(3\alpha\sigma_{pp}^{2(0)} - 4H\alpha\beta^2\sigma_{qp}^{2(0)} + 3H^2\beta^3\sigma_{qq}^{2(0)})}{48\nu^3H^7\alpha^2\beta^3}\right)\right] \times e^{-\left(\alpha H + \lambda\frac{3\alpha\sigma_{pp}^{2(0)} - 4H\alpha\beta^2\sigma_{qp}^{2(0)} + 3H^2\beta^3\sigma_{qq}^{2(0)}}{8\nu^2H^4\alpha\beta^2}\right)t} + \left[\lambda\left(\frac{\sigma_{pp}^{2(0)}(-3\alpha\sigma_{pp}^{2(0)} + 4H\alpha\beta^2\sigma_{qp}^{2(0)} - 3H^2\beta^3\sigma_{qq}^{2(0)})}{32\nu^3H^7\alpha\beta^4}\right)\right] e^{-\left(\beta H - \lambda\frac{3\alpha\sigma_{pp}^{2(0)} - 4H\alpha\beta^2\sigma_{qp}^{2(0)} + 3H^2\beta^3\sigma_{qq}^{2(0)}}{8\nu^2H^4\alpha\beta^2}\right)t}, \tag{B2b}$$

$$\langle q(0,\mathbf{x})p(t,\mathbf{x})\rangle = \left[\lambda\left(\frac{\sigma_{qq}^{(0)}(3\alpha\sigma_{pp}^{2(0)} - 4H\alpha\beta^2\sigma_{qp}^{2(0)} + 3H^2\beta^3\sigma_{qq}^{2(0)})}{32\nu^3H^5\alpha^2\beta}\right)\right] e^{-\left(\alpha H + \lambda\frac{3\alpha\sigma_{pp}^{2(0)} - 4H\alpha\beta^2\sigma_{qp}^{2(0)} + 3H^2\beta^3\sigma_{qq}^{2(0)}}{8\nu^2H^4\alpha\beta^2}\right)t} + \left[\frac{\sigma_{qp}^{2(0)}}{3H} + \lambda\left(\frac{\sigma_{qp}^{2(1)}}{3H} + \frac{(\nu\sigma_{pp}^{2(0)} + H^2\beta^3\sigma_{qq}^{2(0)})(3\alpha\sigma_{pp}^{2(0)} - 4H\alpha\beta^2\sigma_{qp}^{2(0)} + 3H^2\beta^3\sigma_{qq}^{2(0)})}{48\nu^3H^7\alpha\beta^4}\right)\right] \times e^{-\left(\beta H - \lambda\frac{3\alpha\sigma_{pp}^{2(0)} - 4H\alpha\beta^2\sigma_{qp}^{2(0)} + 3H^2\beta^3\sigma_{qq}^{2(0)}}{8\nu^2H^4\alpha\beta^2}\right)t}, \tag{B2c}$$

$$\langle p(0,\mathbf{x})p(t,\mathbf{x})\rangle = \left[\lambda\left(\frac{\sigma_{qp}^{2(0)}(-3\alpha\sigma_{pp}^{2(0)} + 4H\alpha\beta^2\sigma_{qp}^{2(0)} - 3H^2\beta^3\sigma_{qq}^{2(0)})}{48\nu^3H^5\alpha\beta}\right)\right] e^{-\left(\alpha H + \lambda\frac{3\alpha\sigma_{pp}^{2(0)} - 4H\alpha\beta^2\sigma_{qp}^{2(0)} + 3H^2\beta^3\sigma_{qq}^{2(0)}}{8\nu^2H^4\alpha\beta^2}\right)t} + \left[\frac{\sigma_{pp}^{2(0)}}{2H\beta} + \lambda\left(\frac{\sigma_{pp}^{2(1)}}{2H\beta} + \frac{(3\nu\sigma_{pp}^{2(0)} + H\beta^2\alpha\sigma_{qp}^{2(0)})(3\alpha\sigma_{pp}^{2(0)} - 4H\alpha\beta^2\sigma_{qp}^{2(0)} + 3H^2\beta^3\sigma_{qq}^{2(0)})}{48\nu^3H^6\alpha\beta^4}\right)\right] \times e^{-\left(\beta H - \lambda\frac{3\alpha\sigma_{pp}^{2(0)} - 4H\alpha\beta^2\sigma_{qp}^{2(0)} + 3H^2\beta^3\sigma_{qq}^{2(0)}}{8\nu^2H^4\alpha\beta^2}\right)t} \tag{B2d}$$

and their spacelike counterparts are

$$\langle q(t,\mathbf{0})q(t,\mathbf{x})\rangle = \left[\frac{\sigma_{qq}^{2(0)}}{2H\alpha} + \lambda\left(\frac{\sigma_{qq}^{2(1)}}{2H\alpha} + \frac{(3\alpha\sigma_{pp}^{2(0)} - 4H\alpha\beta^2\sigma_{qp}^{2(0)} + 3H^2\beta^3\sigma_{qq}^{2(0)})(3\alpha\sigma_{qp}^{2(0)} - 3\nu H\beta\sigma_{qq}^{2(0)})}{48\nu^3H^7\alpha^3\beta^3}\right)\right] \times |Ha(t)\mathbf{x}|^{-2\alpha - \lambda\frac{3\alpha\sigma_{pp}^{2(0)} - 4H\alpha\beta^2\sigma_{qp}^{2(0)} + 3H^2\beta^3\sigma_{qq}^{2(0)}}{4\nu^2H^5\alpha\beta^2}} + \left[\lambda\left(\frac{\sigma_{qp}^{2(0)}(-3\alpha\sigma_{pp}^{2(0)} + 4H\alpha\beta^2\sigma_{qp}^{2(0)} - 3H^2\beta^3\sigma_{qq}^{2(0)})}{24\nu^3H^7\alpha\beta^3}\right)\right]|Ha(t)\mathbf{x}|^{-3}, \tag{B3a}$$

$$\begin{aligned}\langle q(t,\mathbf{0})p(t,\mathbf{x})\rangle &= \langle p(t,\mathbf{0})q(t,\mathbf{x})\rangle \\ &= \left[\lambda\left(\frac{\sigma_{qq}^{2(0)}(-3\alpha\sigma_{pp}^{2(0)} + 4H\alpha\beta^2\sigma_{qp}^{2(0)} - 3H^2\beta^3\sigma_{qq}^{2(0)})}{32\nu^3H^5\alpha^2\beta}\right)\right]|Ha(t)\mathbf{x}|^{-2\alpha - \lambda\frac{3\alpha\sigma_{pp}^{2(0)} - 4H\alpha\beta^2\sigma_{qp}^{2(0)} + 3H^2\beta^3\sigma_{qq}^{2(0)}}{4\nu^2H^5\alpha\beta^2}} \\ &+ \left[\lambda\left(\frac{\sigma_{pp}^{2(0)}(-3\alpha\sigma_{pp}^{2(0)} + 4H\alpha\beta^2\sigma_{qp}^{2(0)} - 3H^2\beta^3\sigma_{qq}^{2(0)})}{32\nu^3H^7\alpha\beta^4}\right)\right]|Ha(t)\mathbf{x}|^{-2\beta + \lambda\frac{3\alpha\sigma_{pp}^{2(0)} - 4H\alpha\beta^2\sigma_{qp}^{2(0)} + 3H^2\beta^3\sigma_{qq}^{2(0)}}{4\nu^2H^5\alpha\beta^2}} \\ &+ \left[\frac{\sigma_{qp}^{2(0)}}{3H} + \lambda\left(\frac{\sigma_{qp}^{2(1)}}{3H} + \frac{(\sigma_{pp}^{2(0)} + H^2\beta^2\sigma_{qq}^{2(0)})(3\alpha\sigma_{pp}^{2(0)} - 4H\alpha\beta^2\sigma_{qp}^{2(0)} + 3H^2\beta^3\sigma_{qq}^{2(0)})}{48\nu^3H^7\alpha\beta^3}\right)\right]|Ha(t)\mathbf{x}|^{-3},\end{aligned} \tag{B3b}$$

$$\langle p(t,\mathbf{0})p(t,\mathbf{x})\rangle = \left[\frac{\sigma_{pp}^{2(0)}}{2H\beta} + \lambda\left(\frac{\sigma_{pp}^{2(1)}}{2H\beta} + \frac{(3\nu\sigma_{pp}^{2(0)} + 3H\beta^2\sigma_{qp}^{2(0)})(3\alpha\sigma_{pp}^{2(0)} - 4H\alpha\beta^2\sigma_{qp}^{2(0)} + 3H^2\beta^3\sigma_{qq}^{2(0)})}{48\nu^3H^6\alpha\beta^4}\right)\right] \times |Ha(t)\mathbf{x}|^{-2\beta + \lambda\frac{3\alpha\sigma_{pp}^{2(0)} - 4H\alpha\beta^2\sigma_{qp}^{2(0)} + 3H^2\beta^3\sigma_{qq}^{2(0)}}{4\nu^2H^5\alpha\beta^2}} \times \left[\lambda\left(\frac{\sigma_{qp}^{2(0)}(-3\alpha\sigma_{pp}^{2(0)} + 4H\alpha\beta^2\sigma_{qp}^{2(0)} - 3H^2\beta^3\sigma_{qq}^{2(0)})}{24\nu^3H^5\alpha\beta}\right)\right]|Ha(t)\mathbf{x}|^{-3}. \tag{B3c}$$

Substituting these expressions into Eq. (40), we obtain an expression for the $\phi - \phi$ stochastic correlator up to first order in λ. The timelike version is

$$
\begin{aligned}
\langle\phi(0,\mathbf{x})\phi(t,\mathbf{x})\rangle = {} & \frac{1}{1-\frac{\alpha}{\beta}}\Bigg[\frac{\sigma_{qq}^{2(0)}}{2H\alpha} - \frac{\sigma_{qp}^{2(0)}}{3H^2\beta} + \lambda\Bigg(\frac{\sigma_{qq}^{2(1)}}{2H\alpha} - \frac{\sigma_{qp}^{2(1)}}{3H^2\beta} + (2H\alpha^4\beta\sigma_{qp}^{2(0)}(-3\sigma_{pp}^{2(0)} + 4H\beta^2\sigma_{qp}^{2(0)}) \\
& + 9H^4\beta^7\left(\sigma_{qq}^{2(0)}\right)^2 + 9H^2\alpha\beta^4\sigma_{qq}^{2(0)}\left(-\sigma_{pp}^{2(0)} + 2H\beta^2\left(\sigma_{qp}^{2(0)} + H\sigma_{qq}^{2(0)}\right)\right) \\
& - 3\alpha^3\left(6\left(\sigma_{pp}^{2(0)}\right)^2 + 6H^3\beta^4\sigma_{qp}^{2(0)}\sigma_{qq}^{2(0)} - H\beta^2\sigma_{pp}^{2(0)}\left(8\sigma_{qp}^{2(0)} + 3H\sigma_{qq}^{2(0)}\right)\right) \\
& + H\alpha^2\beta^3\left(6\sigma_{pp}^{2(0)}\sigma_{qp}^{2(0)} + H\beta^2\left(-8(\sigma_{qp}^{2(0)})^2 - 24H\sigma_{qp}^{2(0)}\sigma_{qq}^{2(0)} + 9H^2\left(\sigma_{qq}^{2(0)}\right)^2\right)\right)\Big)/(288\nu^3H^8\alpha^3\beta^4)\Bigg)\Bigg] \\
& \times e^{-\left(\alpha H + \lambda\frac{3\alpha\sigma_{pp}^{2(0)} - 4H\alpha\beta^2\sigma_{qp}^{2(0)} + 3H^2\beta^3\sigma_{qq}^{2(0)}}{8\nu^2H^4\alpha\beta^2}\right)t} \\
& + \frac{1}{1-\frac{\alpha}{\beta}}\Bigg[\frac{\sigma_{pp}^{2(0)}}{2H^3\beta^3} - \frac{\sigma_{qp}^{2(0)}}{3H^2\beta} + \lambda\Bigg(\frac{\sigma_{pp}^{2(1)}}{2H^3\beta^3} - \frac{\sigma_{qp}^{2(1)}}{3H^2\beta} + (9\alpha(-\alpha^2 + 2\alpha\beta + \beta^2)\left(\sigma_{pp}^{2(0)}\right)^2 \\
& + 6H\alpha\beta^2(3\alpha^2 - 4\alpha\beta - 3\beta^2)\sigma_{qp}^{2(0)}\sigma_{pp}^{2(0)} + 6H^3\beta^5(\alpha^2 + 4\alpha\beta - \beta^2)\sigma_{qp}^{2(0)}\sigma_{qq}^{2(0)} - 18H^4\beta^7\left(\sigma_{qq}^{2(0)}\right)^2 \\
& + H^2\beta^3(\beta^2 - \alpha^2)(8\alpha\beta(\sigma_{qp}^{2(0)})^2 + 9\sigma_{pp}^{2(0)}\sigma_{qq}^{2(0)}))/(288\nu^3H^8\alpha\beta^6)\Bigg)\Bigg] e^{-\left(\beta H - \lambda\frac{3\alpha\sigma_{pp}^{2(0)} - 4H\alpha\beta^2\sigma_{qp}^{2(0)} + 3H^2\beta^3\sigma_{qq}^{2(0)}}{8\nu^2H^4\alpha\beta^2}\right)t}
\end{aligned}
\tag{B4}
$$

while the spacelike version is

$$
\begin{aligned}
\langle\phi(t,\mathbf{0})\phi(t,\mathbf{x})\rangle = {} & \frac{1}{1-\frac{\alpha}{\beta}}\left[\frac{\sigma_{qq}^{2(0)}}{2H\alpha} + \lambda\left(\frac{\sigma_{qq}^{2(1)}}{2H\alpha} + \frac{(H\beta(3\alpha-\beta)\sigma_{qq}^{2(0)} + 2\alpha\sigma_{qp}^{2(0)})(3\alpha\sigma_{pp}^{2(0)} - 4H\alpha\beta^2\sigma_{qp}^{2(0)} + 3H^2\beta^3\sigma_{qq}^{2(0)})}{32\nu^3H^7\alpha^3\beta^3}\right)\right] \\
& \times |Ha(t)\mathbf{x}|^{-2\alpha - \lambda\frac{3\alpha\sigma_{pp}^{2(0)} - 4H\alpha\beta^2\sigma_{qp}^{2(0)} + 3H^2\beta^3\sigma_{qq}^{2(0)}}{4\nu^2H^5\alpha\beta^2}} \\
& + \frac{1}{1-\frac{\alpha}{\beta}}\left[\frac{\sigma_{pp}^{2(0)}}{2H^3\beta^3} + \lambda\left(\frac{\sigma_{pp}^{2(1)}}{2H^3\beta^3} + \frac{((3\beta-\alpha)\sigma_{pp}^{2(0)} + 2H\beta^2\sigma_{qp}^{2(0)})(3\alpha\sigma_{pp}^{2(0)} - 4H\alpha\beta^2\sigma_{qp}^{2(0)} + 3H^2\beta^3\sigma_{qq}^{2(0)})}{32\nu^3H^8\alpha\beta^6}\right)\right] \\
& \times |Ha(t)\mathbf{x}|^{-2\beta + \lambda\frac{3\alpha\sigma_{pp}^{2(0)} - 4H\alpha\beta^2\sigma_{qp}^{2(0)} + 3H^2\beta^3\sigma_{qq}^{2(0)}}{4\nu^2H^5\alpha\beta^2}} \\
& + \frac{1}{1-\frac{\alpha}{\beta}}\Bigg[-\frac{2\sigma_{qp}^{2(0)}}{3H^2\beta} + \lambda\Bigg(-\frac{2\sigma_{qp}^{2(1)}}{3H^2\beta} + \Big(2H\alpha^2\beta\sigma_{qp}^{2(0)}\left(4H\beta^2\sigma_{qp}^{2(0)} - 3\sigma_{pp}^{2(0)}\right) \\
& - 3H^2\beta^3\sigma_{qq}^{2(0)}\left(3\sigma_{pp}^{2(0)} + H\beta^2\left(2\sigma_{qp}^{2(0)} + 3H\sigma_{qq}^{2(0)}\right)\right) - \alpha\Big(9\left(\sigma_{pp}^{2(0)}\right)^2 - 3H\beta^2\sigma_{pp}^{2(0)}\left(2\sigma_{qp}^{2(0)} - 3H\sigma_{qq}^{2(0)}\right) \\
& - 2H^2\beta^4\sigma_{qp}^{2(0)}\left(4\sigma_{qp}^{2(0)} + 3H\sigma_{qq}^{2(0)}\right)\Big)\Big)\Big/(72\nu^3H^8\alpha\beta^4)\Bigg)\Bigg]|Ha(t)\mathbf{x}|^{-3}.
\end{aligned}
\tag{B5}
$$

This reduces to Eq. (54) if we use the free noise amplitudes (41).

[1] N. D. Birrell and P. C. W. Davies, *Quantum Fields in Curved Space*, Cambridge Monographs on Mathematical Physics (Cambridge University Press, Cambridge, England, 1984).

[2] T. S. Bunch and P. C. W. Davies, Quantum field theory in de Sitter space: Renormalization by point-splitting, Proc. R. Soc. A **360**, 117 (1978).

[3] E. A. Tagirov, Consequences of field quantization in de Sitter type cosmological models, Ann. Phys. (N.Y.) **76**, 561 (1973).
[4] N. A. Chernikov and E. A. Tagirov, Quantum theory of scalar field in de Sitter space-time, Ann. Inst. Henri Poincare **9**, 109 (1968).
[5] A. A. Starobinsky, A new type of isotropic cosmological models without singularity, Phys. Lett. **91B**, 99 (1980).
[6] A. H. Guth, Inflationary universe: A possible solution to the horizon and flatness problems, Phys. Rev. D **23**, 347 (1981).
[7] A. D. Linde, A new inflationary universe scenario: A possible solution of the horizon, flatness, homogeneity, isotropy and primordial monopole problems, Phys. Lett. **108B**, 389 (1982).
[8] A. R. Liddle and D. H. Lyth, *Cosmological Inflation and Large Scale Structure* (Cambridge University Press, Cambridge, England, 2000).
[9] J. A. Vazquez Gonzalez, L. E. Padilla, and T. Matos, Inflationary cosmology: From theory to observations, Rev. Mex. Fís. E **17**, 73 (2020).
[10] D. Baumann, *Cosmology* (Cambridge University Press, Cambridge, England, 2022).
[11] M. Sasaski, Large scale quantum fluctuations in the inflationary Universe, Prog. Theor. Phys. **76**, 1036 (1986).
[12] A. Linde and V. Mukhanov, Non-Gaussian isocurvature perturbations from inflation, Phys. Rev. D **56**, R535 (1997).
[13] S. M. Leach, M. Sasaki, D. Wands, and A. R. Liddle, Enhancement of superhorizon scale inflationary curvature perturbations, Phys. Rev. D **64**, 023512 (2001).
[14] P. J. E. Peebles and A. Vilenkin, Noninteracting dark matter, Phys. Rev. D **60**, 103506 (1999).
[15] W. Hu, R. Barkana, and A. Gruzinov, Fuzzy Cold Dark Matter: The Wave Properties of Ultralight Particles, Phys. Rev. Lett. **85**, 1158 (2000).
[16] T. Markkanen, A. Rajantie, and T. Tenkanen, Spectator dark matter, Phys. Rev. D **98**, 123532 (2018).
[17] L. Jukko and A. Rajantie, Stochastic isocurvature constraints for axion dark matter with high-scale inflation, arXiv:2107.07948.
[18] J. R. Espinosa, G. F. Giudice, and A. Riotto, Cosmological implications of the Higgs mass measurement, J. Cosmol. Astropart. Phys. 05 (2008) 002.
[19] M. Herranen, T. Markkanen, S. Nurmi, and A. Rajantie, Spacetime Curvature and the Higgs Stability During Inflation, Phys. Rev. Lett. **113**, 211102 (2014).
[20] T. Markkanen, A. Rajantie, and S. Stopyra, Cosmological aspects of Higgs vacuum metastability, Front. Astron. Space Sci. **5**, 40 (2018).
[21] J. E. Camargo-Molina and A. Rajantie, Phase transitions in de Sitter: The stochastic formalism, arXiv:2204.02875.
[22] J. E. Camargo-Molina, M. C. González, and A. Rajantie, Phase transitions in de Sitter: Quantum corrections, arXiv:2204.03480.
[23] L. Bethke, D. G. Figueroa, and A. Rajantie, Anisotropies in the Gravitational Wave Background from Preheating, Phys. Rev. Lett. **111**, 011301 (2013).
[24] B. Allen and A. Folacci, Massless minimally coupled scalar field in de Sitter space, Phys. Rev. D **35**, 3771 (1987).
[25] B. Allen, Vacuum states in de Sitter space, Phys. Rev. D **32**, 3136 (1985).
[26] M. Sasaki, H. Suzuki, K. Yamamoto, and J. Yokoyama, Superexpansionary divergence: Breakdown of perturbative quantum field theory in space-time with accelerated expansion, Classical Quantum Gravity **10**, L55 (1993).
[27] H. Suzuki, M. Sasaki, K. Yamamoto, and J. Yokoyama, Probability distribution functional for equal time correlation functions in curved space, Int. J. Mod. Phys. A **09**, 221 (1994).
[28] B. L. Hu and D. J. O'Connor, Symmetry behavior in curved spacetime: Finite-size effect and dimensional reduction, Phys. Rev. D **36**, 1701 (1987).
[29] D. Boyanovsky, H. J. de Vega, and N. G. Sanchez, Quantum corrections to slow roll inflation and new scaling of superhorizon fluctuations, Nucl. Phys. **B747**, 25 (2006).
[30] J. Serreau, Effective Potential for Quantum Scalar Fields in a de Sitter Geometry, Phys. Rev. Lett. **107**, 191103 (2011).
[31] T. Arai, Nonperturbative infrared effects for light scalar fields in de Sitter space, Classical Quantum Gravity **29**, 215014 (2012).
[32] F. Gautier and J. Serreau, Infrared dynamics in de Sitter space from Schwinger–Dyson equations, Phys. Lett. B **727**, 541 (2013).
[33] M. Herranen, T. Markkanen, and A. Tranberg, Quantum corrections to scalar field dynamics in a slow-roll spacetime, J. High Energy Phys. 05 (2014) 026.
[34] F. Gautier and J. Serreau, Scalar field correlator in de Sitter space at next-to-leading order in a $1/N$ expansion, Phys. Rev. D **92**, 105035 (2015).
[35] M. Guilleux and J. Serreau, Quantum scalar fields in de Sitter space from the nonperturbative renormalization group, Phys. Rev. D **92**, 084010 (2015).
[36] D. Boyanovsky, Effective field theory during inflation: Reduced density matrix and its quantum master equation, Phys. Rev. D **92**, 023527 (2015).
[37] M. Guilleux and J. Serreau, Nonperturbative renormalization group for scalar fields in de Sitter space: Beyond the local potential approximation, Phys. Rev. D **95**, 045003 (2017).
[38] D. Boyanovsky, Effective field theory during inflation. II. Stochastic dynamics and power spectrum suppression, Phys. Rev. D **93**, 043501 (2016).
[39] D. L. Nacir, F. D. Mazzitelli, and L. G. Trombetta, To the sphere and back again: De Sitter infrared correlators at NTLO in $1/N$, J. High Energy Phys. 08 (2019) 052.
[40] A. A. Starobinsky, Stochastic de Sitter (inflationary) stage in the early universe, Lect. Notes Phys. **246**, 107 (1986).
[41] A. A. Starobinsky and J. Yokoyama, Equilibrium state of a self-interacting scalar field in the de Sitter background, Phys. Rev. D **50**, 6357 (1994).
[42] N. C. Tsamis and R. P. Woodard, Stochastic quantum gravitational inflation, Nucl. Phys. **B724**, 295 (2005).
[43] F. Finelli, G. Marozzi, A. A. Starobinsky, G. P. Vacca, and G. Venturi, Generation of fluctuations during inflation: Comparison of stochastic and field-theoretic approaches, Phys. Rev. D **79**, 044007 (2009).
[44] F. Finelli, G. Marozzi, A. A. Starobinsky, G. P. Vacca, and G. Venturi, Stochastic growth of quantum fluctuations during slow-roll inflation, Phys. Rev. D **82**, 064020 (2010).
[45] V. Vennin and A. A. Starobinsky, Correlation functions in stochastic inflation, Eur. Phys. J. C **75**, 413 (2015).

[46] R. J. Hardwick, V. Vennin, C. T. Byrnes, J. Torrado, and D. Wands, The stochastic spectator, J. Cosmol. Astropart. Phys. 10 (2017) 018.
[47] J. Tokuda and T. Tanaka, Statistical nature of infrared dynamics on de Sitter background, J. Cosmol. Astropart. Phys. 02 (2018) 014.
[48] J. Tokuda and T. Tanaka, Can all the infrared secular growth really be understood as increase of classical statistical variance?, J. Cosmol. Astropart. Phys. 11 (2018) 022.
[49] D. Glavan, T. Prokopec, and A. A. Starobinsky, Stochastic dark energy from inflationary quantum fluctuations, Eur. Phys. J. C **78**, 371 (2018).
[50] D. Cruces, C. Germani, and T. Prokopec, Failure of the stochastic approach to inflation beyond slow-roll, J. Cosmol. Astropart. Phys. 03 (2019) 048.
[51] J. Grain and V. Vennin, Stochastic inflation in phase space: Is slow roll a stochastic attractor?, J. Cosmol. Astropart. Phys. 05 (2017) 045.
[52] H. Firouzjahi, A. Nassiri-Rad, and M. Noorbala, Stochastic ultra slow roll inflation, J. Cosmol. Astropart. Phys. 01 (2019) 040.
[53] L. Pinol, S. Renaux-Petel, and Y. Tada, Inflationary stochastic anomalies, Classical Quantum Gravity **36**, 07LT01 (2019).
[54] R. J. Hardwick, T. Markkanen, and S. Nurmi, Renormalisation group improvement in the stochastic formalism, J. Cosmol. Astropart. Phys. 09 (2019) 023.
[55] C. Pattison, V. Vennin, H. Assadullahi, and D. Wands, Stochastic inflation beyond slow roll, J. Cosmol. Astropart. Phys. 07 (2019) 031.
[56] G. Moreau and J. Serreau, Unequal time correlators of stochastic scalar fields in de Sitter space, Phys. Rev. D **101**, 045015 (2020).
[57] G. Moreau and J. Serreau, $1/n$ expansion for stochastic fields in de Sitter spacetime, Phys. Rev. D **102**, 125015 (2020).
[58] G. Rigopoulos, Thermal interpretation of infrared dynamics in de Sitter, J. Cosmol. Astropart. Phys. 07 (2016) 035.
[59] I. Moss and G. Rigopoulos, Effective long wavelength scalar dynamics in de Sitter, J. Cosmol. Astropart. Phys. 05 (2017) 009.
[60] T. Prokopec and G. Rigopoulos, Functional renormalization group for stochastic inflation, J. Cosmol. Astropart. Phys. 08 (2018) 013.
[61] M. Bounakis and G. Rigopoulos, Feynman rules for stochastic inflationary correlators, J. Cosmol. Astropart. Phys. 05 (2020) 046.
[62] B. Garbrecht, G. Rigopoulos, and Y. Zhu, Infrared correlations in de Sitter space: Field theoretic versus stochastic approach, Phys. Rev. D **89**, 063506 (2014).
[63] B. Garbrecht, F. Gautier, G. Rigopoulos, and Y. Zhu, Feynman diagrams for stochastic inflation and quantum field theory in de Sitter space, Phys. Rev. D **91**, 063520 (2015).
[64] M. Morikawa, Dissipation and fluctuation of quantum fields in expanding universes, Phys. Rev. D **42**, 1027 (1990).
[65] G. Rigopoulos, Fluctuation-dissipation and equilibrium for scalar fields in de Sitter, arXiv:1305.0229.
[66] L. P. Levasseu, Lagrangian formulation of stochastic inflation: Langevin equations, one-loop corrections and a proposed recursive approach, Phys. Rev. D **88**, 083537 (2013).
[67] L. Pinol, S. Renaux-Petel, and Y. Tada, A manifestly covariant theory of multifield stochastic inflation in phase space: Solving the discretisation ambiguity in stochastic inflation, J. Cosmol. Astropart. Phys. 04 (2021) 048.
[68] G. Rigopoulos and A. Wilkins, Inflation is always semi-classical: Diffusion domination overproduces primordial black holes, J. Cosmol. Astropart. Phys. 12 (2021) 027.
[69] J. O. Andersen, M. Eriksson, and A. Tranberg, Stochastic inflation from quantum field theory and the parametric dependence of the effective noise amplitude, J. High Energy Phys. 02 (2022) 121.
[70] T. Markkanen, A. Rajantie, S. Stopyra, and T. Tenkanen, Scalar correlation functions in de Sitter space from the stochastic spectral expansion, J. Cosmol. Astropart. Phys. 08 (2019) 001.
[71] T. Markkanen and A. Rajantie, Scalar correlation functions for a double-well potential in de Sitter space, J. Cosmol. Astropart. Phys. 03 (2020) 049.
[72] A. Cable and A. Rajantie, Free scalar correlators in de Sitter space via the stochastic approach beyond the slow-roll approximation, Phys. Rev. D **104**, 103511 (2021).
[73] A. Cable and A. Rajantie (to be published).